https://doi.org/10.5194/egusphere-2025-2684
Preprint. Discussion started: 15 July 2025

Evaluating Precipitation Behavior in CESM2 Using Nudging Technique

Fucheng Yang[1], Jie He[1], Boniface Fosu[2], Yen-Heng Lin[2], and Yi Deng[1]

[1]School of Earth and Atmospheric Sciences, Georgia Institute of Technology, Atlanta, Georgia, USA
[2]Department of Geosciences, Mississippi State University, Starkville, Mississippi, USA

Correspondence: Fucheng Yang (fyang368@gatech.edu)

Abstract. Persistent precipitation biases in coupled general circulation models (CGCMs) are often linked to deficiencies in moist physics parameterizations and their interactions with large-scale dynamics. However, disentangling these effects is challenging due to the coupling between precipitation and the large-scale environment. Nudging—a simulation technique that forces model variables toward a target state—offers a means to isolate parameterization errors. This study explores and improves the nudging implementation in the Community Earth System Model (CESM) version 2.2.2, and evaluates the performance of precipitation by nudging horizontal wind, moisture, and/or temperature toward reanalysis. We identify a limitation in the default nudging sequence, where separating the computation and application of nudging tendencies by moist processes leads to artificial precipitation biases. A revised implementation significantly reduces these errors, establishing a more robust framework for parameterization evaluation. Using this optimized setup, we show that forcing model with observed horizontal wind improves mean precipitation by enhancing low-level convergence in the Pacific warm pool and ITCZ, while reducing the wet bias in the subtropics. Nonetheless, the model continues to produce excessive drizzle and insufficient heavy precipitation, with rainy-hour relative humidity exceeding reanalysis values. Nudging temperature or specific humidity offers limited additional improvement. These results reveal an intrinsic inefficiency in converting moisture into heavy precipitation—independent of large-scale state errors—highlighting a fundamental weakness in the model's parameterizations. This study also underscores the value of nudging for isolating parameterization deficiencies in model evaluation.

https://doi.org/10.5194/egusphere-2025-2684
Preprint. Discussion started: 15 July 2025

1 Introduction

The double-Intertropical Convergence Zone (ITCZ) problem has persisted across generations of coupled general circulation models (CGCMs) (Mechoso et al., 1995; Lin, 2007; Zhang et al., 2015; Li and Xie, 2014; Zhang et al., 2019; Fiedler et al., 2020). This model-simulated double-ITCZ manifests as two pronounced rain bands straddling the equator over the central and eastern tropical Pacific, contrast to a single strong rain-band north of the equator and a weaker, transient one south of the equator only in boreal spring in observation. While the extratropical effects have been found to play a relatively minor role (Kang et al., 2008; Hwang and Frierson, 2013; Kay et al., 2016; Hawcroft et al., 2017), warmer southeastern Pacific due to reduced marine stratocumulus clouds (Ma et al., 1996; Yu and Mechoso, 1999; Gordon et al., 2000; Song and Zhang, 2016; Woelfle et al., 2019; Zhou et al., 2022) and overly frequent deep convection within the descending branch of the Walker circulation (Bony et al., 2004; Zhang and Wang, 2006; Song and Zhang, 2009, 2025) are considered more important. These two mechanisms are often associated with too frequent drizzle and light precipitation, and hence are linked to precipitation parameterizations in climate models.

The goal of precipitation parameterizations is to emulate rainfall given inputs of large-scale (*i.e.*, the grid box scale) variables such as winds, moisture, and temperature, while also feeding back to the large-scale environment through latent heat release, cloud-radiative interactions, etc. While the representation of the ITCZ and precipitation in general is most likely affected by model's parameterizations, such as convection and stratocumulus schemes, how do we evaluate such an effect? A common approach is to tinker with specific elements of the model's parameterization schemes and observe its impacts on the simulated features like the ITCZ, such as the closure of convection scheme in Song and Zhang (2025). However, due to the tight coupling between precipitation and the large-scale variables in models, fixating exclusively on a specific aspect of parameterizations may be counterproductive. The precipitation bias is likely rooted in errors in both the parameterization schemes and their interactions with the broader environment. Attempts to correct the parameterization schemes in a model that already simulates a biased large-scale environment may result in overaccommodation—an improvement in the ITCZ at the expense of undermining other aspects of the simulated climate, as seen in Song and Zhang (2025).

The first primary goal of this paper is to assess the performance of precipitation parameterizations in a global climate model where its large-scale variables are adjusted to match the reanalysis. Our underlying premise is that 1) model biases, such as the double-ITCZ problem, result from a multitude of model imperfections, and 2) a good model parameterization is able to emulate the observed precipitation given correct input variables but should not be expected to perform well in a model with a biased large-scale climate. We aim to develop and evaluate a modeling framework commonly known as nudging. It allows one to correct a model's large-scale environment, thus providing an ideal testbed for parameterizations.

Now we provide a brief review of nudging, mathematically known as Newtonian relaxation, a widely used technique in atmospheric simulations that relaxes meteorological fields toward a target state. Initially, it was employed to generate initial conditions for weather prediction (Hoke and Anthes, 1976). During the preforecast integration, prognostic variables such as horizontal wind and temperature are adjusted toward observed values by introducing an additional tendency term to the partial

https://doi.org/10.5194/egusphere-2025-2684
Preprint. Discussion started: 15 July 2025

differential equations:

$$\frac{\partial A}{\partial t} = \mathcal{M}(A) - G(A - A_{target}), \tag{1}$$

where A is the time-dependent variable, A_{target} is the prescribed target value derived from observations, and G is the nudging coefficient that determines the strength of the nudging. The term $\mathcal{M}(A)$ represents the original dynamical or physical processes native to the model.

With advancements in climate modeling over the recent decades, the application of nudging has expanded beyond initialization to model development and evaluation. The impacts of different nudging schemes have also been widely discussed, including the choice of nudging variables and strength, grid versus spectral nudging, and the stage within the model workflow where nudging is applied (Zhang et al., 2014; Vincent and Hahmann, 2015; Omrani et al., 2015; Lin et al., 2016; Zhang et al., 2022). While nudging horizontal wind is the most common approach in the studies mentioned above (given the critical role of circulation in atmospheric simulations), temperature and specific humidity are also considered, particularly in research on convection, precipitation, and cloud radiative effect. However, the effect of temperature and specific humidity nudging varies by case (Subramanian and Zhang, 2014; Zhang et al., 2014; Ma et al., 2015; Sun et al., 2019). In addition, Zhang et al. (2022) showed that the placement of nudging within the computing sequence significantly affected results in temperature-nudging experiments in the Energy Exascale Earth System Model (E3SM) Atmosphere Model version 1 (EAMv1) (Rasch et al., 2019). They found that modifying the workflow to compute the nudging tendency between adjustment physics and radiation transfer (see Z22 in Fig. 1) substantially improved the consistency between nudging and free-running simulations. However, their studies did not further investigate the effects of specific humidity nudging.

In the Community Earth System Model (CESM) version 2.2.2, a set of nudging routines is available as an optional configuration within the Community Atmosphere Model (CAM) version 6.3. By default, however, CESM2.2.2 applies nudging in a way similar to that described by Zhang et al. (2022), which has been proven problematic in EAMv1. When using this default nudging approach, systematic biases emerge even when the model is nudged toward its own climate, as will be further discussed in Section 3.1. This motivates **the second primary goal** of this study: to explore alternative nudging schemes in CESM2.2.2 and evaluate their impacts on simulating the hydrological cycle, with a focus on precipitation.

The remainder of the paper is organized as follows. Section 2 describes the observational and reanalysis data used in this study, details the model setup, and outlines modifications to the nudging computing sequence. In Section 3, an optimal nudging scheme is proposed based on a process-by-process analysis of the model's temporal evolution, and the precipitation bias induced by the parameterization schemes is examined. Finally, Section 4 summarizes the findings and discusses potential improvements in model's precipitation parameterizations.

https://doi.org/10.5194/egusphere-2025-2684
Preprint. Discussion started: 15 July 2025

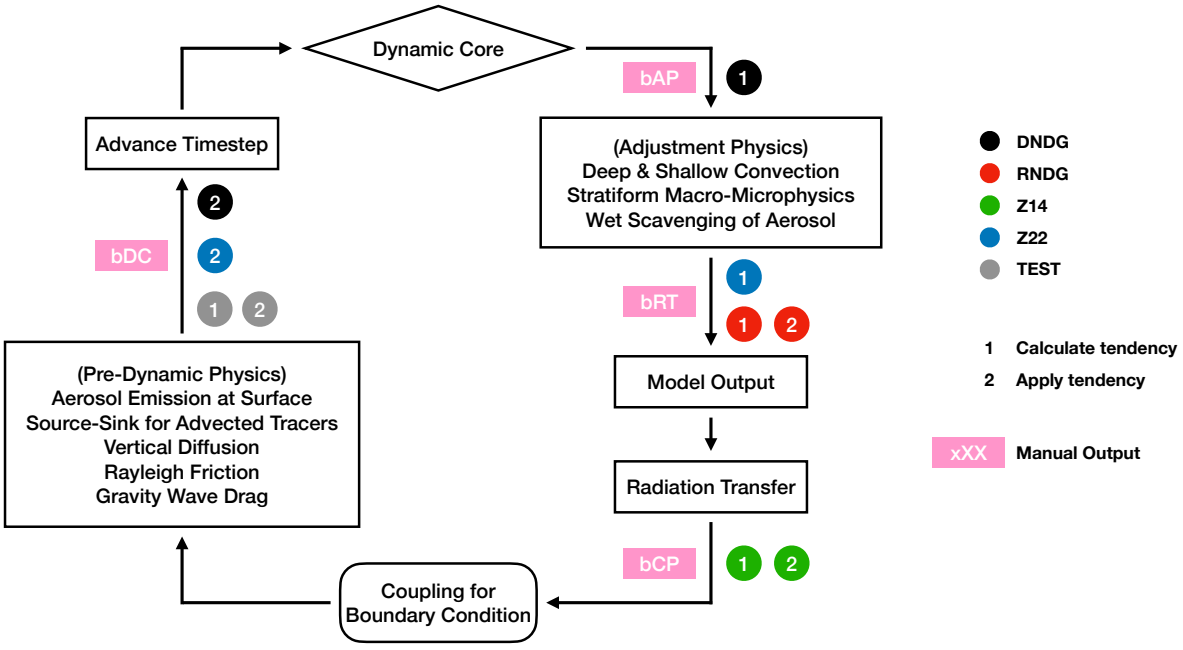

Figure 1. Flowchart illustrating the implementation of nudging within the computing sequence. The colored circles indicate the points where the nudging is computed (denoted by number "1") and applied (denoted by number "2") under different nudging schemes: the default nudging in CESM2.2.2 (DNDG, black), the revised nudging suggested in this study (RNDG, red), the approach used in Zhang et al. (2014) (Z14, green), the approach in Zhang et al. (2022) (Z22, blue), and a test configurations (TEST, grey). The pink boxes indicate where model state is print out manually between different processes: the dynamic core, adjustment physics, radiation transfer, and pre-dynamic physics.

2 Data and Method

2.1 Reanalysis and observation

3-hourly horizontal wind (U, V), temperature (T), and specific humidity (Q) data are obtained from the 5th generation of European Centre for Medium-Range Weather Forecasts (ECMWF) Reanalysis (ERA5) (Hersbach et al., 2020). These 4-D variables are assimilated based on balloon, radiosonde, dropsonde and aircraft measurements in ECMWF Integrated Forecasting System (IFS), with observed wind being also obtained from satellite-derived Atmospheric Motion Vectors (AMV). These data have a horizontal resolution of $1^{o} \times 1^{o}$, ranging from 2009-10-01 to 2014-12-31. For use as target data in nudging simulations, they are interpolated to the model grid (approximately $1.25^{o} \times 0.94^{o}$) by area-weighted averaging on grid boxes, and pressure-level variables are transformed to the model's hybrid sigma-pressure coordinate. Surface pressure and thermal radiation at top of atmosphere (outgoing longwave radiation; OLR) are also obtained for comparison.

https://doi.org/10.5194/egusphere-2025-2684
Preprint. Discussion started: 15 July 2025

Precipitation data are obtained from the Global Precipitation Measurement (GPM) Integrated Multi-satellitE Retrievals for GPM (IMERG; half-hourly, $0.1^{\circ} \times 0.1^{\circ}$) (Huffman et al., 2020). IMERG uses inter-calibrated estimates from an international constellation of precipitation-relevant satellites and other data sources to compute precipitation over latitudes from 60°S to 60°N, and partially outside this band. This dataset is also interpolated to the model grid by area-weighted averaging and is summed hourly. Precipitation from ERA5 (hourly, $1^{\circ} \times 1^{\circ}$) is also used for comparison but is presented only in Appendices. This is because ERA5 does not directly assimilate rain gauge data, except over the eastern United States since 2009 (Lavers et al., 2022). Instead, its precipitation is primarily derived from parameterization schemes in IFS, originally developed by Tiedtke (1989).

In analysis on precipitation, distributions are constructed for both frequency and amount at each grid box. The hourly (or daily) precipitation is grouped into bins [10^{-5}, 10^{-4}, 10^{-3}, ... , 10^{3}] mm. Precipitation less than 10^{-5} mm (10^{-4} mm) is characterized as "No Rain" for hourly (daily) accumulated data.

2.2 Nudging

In the current model, the implementation of nudging differs from what Eq. 1 entails. Specifically, the atmospheric model goes through a chain of processes (*e.g.*, dynamic core, adjustment physics, and radiation transfer) within every timestep (see Fig. 1). Upon the completion of each process, the model state is updated. In the default nudging scheme of CESM2.2.2, the nudging term, $G(A - A_{target})$, is computed before the model physics but applied at the end of the integration timestep:

$$\left.\begin{aligned} A_t\big|_{nudging} &= \epsilon\alpha\frac{A_{target} - A_1^*}{\Delta t} \\ A_{NDG} &= A_2^* + \Delta t A_t\big|_{nudging} \end{aligned}\right\}, \tag{2}$$

where $A_t\big|_{nudging}$ is the nudging tendency, A_1^* (A_2^*) is the model state before the computation (application) of nudging tendency, A_{NDG} is the model state after applying nudging tendency, Δt is the model timestep (30 minutes in CESM2.2.2), ϵ is the horizontal and vertical window weighting, and α is the nudging coefficient used in this study, which represents how much bias between A_1^* and A_{target} is corrected by nudging at each timestep. In some previous studies, the nudging strength is also evaluated by the relaxation timescale ($\tau = \Delta t/\alpha$).

Following Sun et al. (2019) and Zhang et al. (2022), the target data has a frequency of 3 hours and is linearly interpolated between two neighboring 3-hour time slices so that nudging is conducted at each model timestep. This frequency is sufficient to capture the diurnal and semi-diurnal timescales. The nudging is applied on the entire atmosphere vertically and horizontally except near the pole by setting a meridionally varying ϵ (see Fig. B1).

2.3 Model setup

In this study, we focus on the implement of nudging in CAM6.3, which is the atmospheric component of CESM2.2.2. In CAM6.3, we use the finite volume dynamical core with a horizontal resolution of approximately $1.25^{\circ} \times 0.94^{\circ}$ with a model time step of 0.5 hour. CAM6.3 employs the Cloud Layers Unified by Binormals (CLUBB) scheme to parameterize the moist

https://doi.org/10.5194/egusphere-2025-2684
Preprint. Discussion started: 15 July 2025

boundary layer, shallow convection, and cloud macrophysics (Golaz et al., 2002; Bogenschutz et al., 2013). An improved two-moment prognostic cloud microphysics (MG2) scheme has also been introduced, which carries prognostic precipitation species—rain and snow—alongside cloud condensates (Gettelman and Morrison, 2015). Additionally, deep convection, as described in Zhang and McFarlane (1995), has been significantly retuned to increase its sensitivity to convective inhibition.

Two sets of simulations, lasting 6 months and 63 months (about 5 years), respectively, are conducted in an Atmospheric Model Intercomparison Project (AMIP)-type framework forced with observed SST (FHIST_BGC), as outlined in Table 1. All simulations begin on 2009-10-01, using a set of identical restart files, and the first 3 months are discarded as spin-up. These simulations are divided into two groups. Group 1 consists a set of baseline simulations (*e.g.*, DNDG_CTL3hr_UVQ), in which the model is nudged toward its own outputs from a free-running simulation (*i.e.*, CTLs) to validate the application of nudging. The degree to which the nudged simulation deviates from CTLs is a good first indicator of the effectiveness of the nudging scheme. If done perfectly, nudging towards itself should result in a simulation that resembles (if not is identical to) the CTLs since the nudging term is always small.

Group 1 starts with a short (6 months) control-run simulation (CTLs), followed by a set of nudged simulations. These nudged simulations differ by their nudging schemes and variables nudged. As shown in Fig. 1, DNDG represents the simulations using the default nudging scheme in CESM2.2.2, where the nudging tendency is computed between the dynamical core and the adjustment physics. RNDG refers to a revised nudging scheme proposed in this study, in which the nudging tendency is both computed and applied after the adjustment physics but before model output. Z14 and Z22 denote the nudging schemes adopted in previous studies by Zhang et al. (2014) and Zhang et al. (2022), respectively. Together with TEST, which computes and applies nudging tendency after the pre-dynamic physics, these schemes highlight two key findings: 1) systematic biases arise when adjustment physics occurs between the computation and application of the nudging tendency (*i.e.*, DNDG versus Z22); and 2) the model shows limited sensitivity to the nudging location within the workflow when the nudging tendency is computed and applied simultaneously (*e.g.*, RNDG, Z14, and TEST). Because horizontal wind is minimally affected by adjustment physics, radiative transfer, and pre-dynamic physics, UV nudging is not performed in Group 1. All outputs from Group 1 are recorded at half-hour intervals.

Group 2 includes a longer (about 5 years) control simulation (CTL) and a set of nudging simulations targeted toward ERA5. Since the topography in CESM2.2.2 is different from ERA5 in regions with significant mountains and the temperature and humidity used as target data is from ERA5 which is sensitive to the elevation and pressure in lower troposphere, all simulations in Group 2 use ERA5's topography. The output from Group 2 includes half-hourly data for single-level variables such as precipitation, and daily data for pressure-level variables. These simulations are designed to assess how the precipitation behavior in the model differs from observations and highlight the biases that remain when the modeled atmosphere is forced toward observations. In both Groups 1 and 2, temperature and specific humidity are not nudged simultaneously. This decision stems from the fact that the CESM2.2.2's troposphere in this AMIP-type simulation is significantly cooler than that of ERA5 (see Fig. 8**a**), and the model's parameters appear to be tuned to adapt its cooler climate. As shown in Fig. 9**e** and supported

https://doi.org/10.5194/egusphere-2025-2684
Preprint. Discussion started: 15 July 2025

Table 1. List of simulations analyzed in this study.

Group	Simulation Short Name	Analysis Period	Topography	Target and Frequency	Workflow	Nudging Variables	Nudging Coefficient (Relaxation Timescale)
1	CTLs	2010/01—2010/03	Default	—	—	—	—
1	DNDG_CTL05hr_UVQ			CTLs 0.5hr	DNDG	UVQ	0.1 (5hr)
1	DNDG_CTL3hr_UVQ			CTLs 3hr	DNDG	UVQ	
1	DNDG_CTL3hr_UVT				DNDG	UVT	
1	RNDG_CTL3hr_UVQ				RNDG	UVQ	
1	RNDG_CTL3hr_UVT				RNDG	UVT	
1	Z14_CTL3hr_UVQ				Z14	UVQ	
1	Z14_CTL3hr_UVT				Z14	UVT	
1	Z22_CTL3hr_UVQ				Z22	UVQ	
1	Z22_CTL3hr_UVT				Z22	UVT	
1	TEST_CTL3hr_UVQ				TEST	UVQ	
1	TEST_CTL3hr_UVT				TEST	UVT	
2	CTL	2010/01—2014/12	ERA5	—	—	—	—
2	RNDG_UV1			ERA5 3hr	RNDG	UV	1 (0.5hr)
2	RNDG_UVQ1					UVQ	1 (0.5hr)
2	RNDG_UVT1					UVT	1 (0.5hr)

by Ma et al. (2015), nudging both temperature and specific humidity leads to unrealistically low precipitation, rendering comparisons with other simulations ineffective.

3 Results

3.1 The optimal nudging scheme for CESM2.2.2

Modern climate models are highly robust, consistently producing identical outputs bit-by-bit when run under the same settings, hardware, and compilers. Nudging introduces an additional tendency term (as shown in Eq. 2) to force the model toward a specified target state, thereby modifying the modeled climate. Ideally, if the target data is the model's own climate, the effect of nudging should be negligible. Any significant bias in this case would indicate that nudging introduces additional errors, potentially undermining the reliability of subsequent analysis. In our baseline simulations—where the model is nudged toward its own 3-hourly outputs from a free-running control run—two primary sources of bias are identified: 1) the linear interpolation of target data (3-hourly) due to the mismatch with the model's timestep (0.5 hour), and 2) the specific way to compute and apply the nudging tendencies. These biases are acceptable only if they are small enough or random enough not to distort the model's climatology. However, if such biases interact nontrivially with model dynamics and lead to substantial

https://doi.org/10.5194/egusphere-2025-2684
Preprint. Discussion started: 15 July 2025

deviations in the simulated climate, the nudging implementation must be considered flawed and unsuitable for isolating physical parameterization effects.

3.1.1 Discrepancy in baseline simulations due to nudging scheme

As shown in Fig. 2**a**, the total precipitation in CTLs peaks in the central and southwestern tropical Pacific, with maximum values exceeding 16 mm/day. The default nudging scheme (*i.e.*, DNDG_CTL3hr_UVQ) is noticeably drier over most mid-latitude oceans and the central tropical Pacific (Fig. 2**c**). For example, over the North Pacific Ocean, deviations reach -0.4 mm/day, accounting for approximately 5% of the 3-month mean precipitation. In the central Pacific, the pattern of negative precipitation bias closely resembles that of the mean precipitation. To assess the impact of target data frequency, we also conducted a nudging simulation in which the target data frequency matches the model timestep (0.5 hour), as shown in Fig. 2**b**. However, this adjustment does not substantially reduce the bias. Furthermore, when temperature is nudged alongside horizontal wind, discrepancies increase, exceeding ± 1 mm/day over many tropical areas (Fig. 2**d**). The pattern of the discrepancies is rather irregular, with a somewhat coherent meridional dipole structure straddling the eastern equatorial Pacific.

In contrast, the precipitation discrepancies between the UVQ simulations and CTLs are substantially reduced under all alternative nudging schemes compared to the default in CESM2.2.2, particularly over tropical oceans (Fig. 2**e**–**h**). For the UVT simulations, random biases are still present (Fig. 2**i**–**l**), but their magnitudes are smaller, and the previously enhanced ITCZ under default nudging is no longer observed. When we use half-hourly output as the target data, precipitation from the RNDG scheme (for both UVQ and UVT) is identical to that of CTLs, and the precipitation biases from Z14, Z22 and TEST are also reduced compared to simulations using 3-hourly target data although not zero (not shown).

These results also demonstrate the effectiveness of nudging in suppressing the internal variability of the model's climate when using a nudging coefficient of 0.1. Different nudging schemes introduce random errors into the modeled climate due to differences in the location where the nudging tendency is computed and applied. However, under the RNDG, Z14, Z22, and TEST nudging schemes, the precipitation biases in the UVQ simulations are nearly identical, and the UVT simulations exhibit similar behavior—namely, spatially random patterns over the tropical Indian Ocean, western tropical Pacific Ocean, and tropical South America. This consistency supports the use of 5-year simulations, which are relatively short, as a reasonable representation of climatological bias in Group 2.

3.1.2 Attribution of discrepancy

The precipitation discrepancies between the baseline simulations and CTLs will be discussed in two parts: 1) differences between the default nudging and the four revised nudging schemes, and 2) differences between UVQ and UVT nudging. As noted in Zhang et al. (2022), the placement of nudging within the computing sequence plays a critical role in EAMv1, which is a descendant of CAM5.0 Rasch et al. (2019). The workflow of CAM6.3 contains four main processes: 1) dynamical core, 2) adjustment physics, which primarily include dry and moist adjustments, 3) radiation transfer, and 4) pre-dynamic physics which include all remaining physics after coupling and before the timestep advance (Fig. 1). The absolute changes in specific

https://doi.org/10.5194/egusphere-2025-2684
Preprint. Discussion started: 15 July 2025

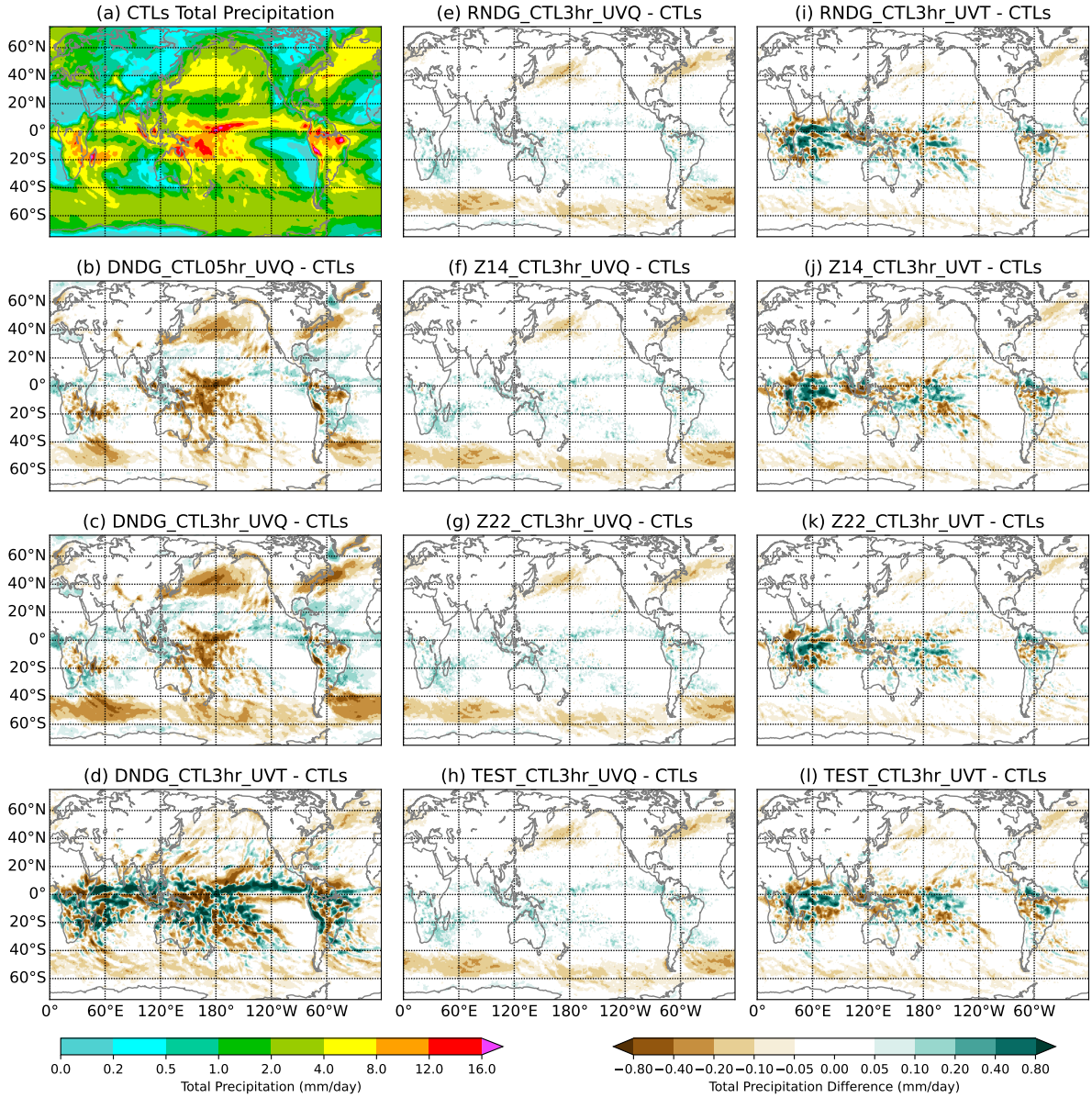

Figure 2. Global pattern of (**a**) the 3-month (from 2010-01-01 to 2010-03-31) climatological precipitation in free-running simulation (CTLs), and (**b–l**) the differences in precipitation between baseline simulations and CTLs.

https://doi.org/10.5194/egusphere-2025-2684
Preprint. Discussion started: 15 July 2025

humidity and temperature at about "859.5 mb" (in model's hybrid sigma-pressure coordinate) due to each process in CTLs are recorded and shown in Fig. 3. Substantial changes in both humidity and temperature occur during the dynamic core and adjustment physics stages, with minimal changes during pre-dynamic physics. Additionally, temperature shows noticeable changes during radiation transfer, though with smaller magnitudes over the tropical Indian Ocean and the central and western tropical Pacific (Fig. 3**g**). In contrast, changes in specific humidity during radiation transfer are identically zero.

We first explain how the pronounced precipitation biases between the default and revised nudging schemes arise with the help of these process-split outputs. In the default nudging configuration of CESM2.2.2, the nudging tendency is computed before adjustment physics but applied after pre-dynamic physics. For instance, in the UVQ simulation, dynamic-induced moist convergence leads to precipitation during adjustment physics, accompanied by a reduction in specific humidity. Under the default nudging scheme, the nudging tendency is computed based on the higher humidity values before adjustment physics. When this tendency is applied after pre-dynamic physics, it removes excessive moisture, over-drying the atmosphere, which results in reduced humidity in the following timestep and consequently suppressing precipitation (Fig. 2**b** and **c**). A similar mechanism operates in the UVT simulation. In the eastern equatorial Pacific ITCZ, strong precipitation is associated with significant adiabatic heating during adjustment physics. If the nudging tendency is computed before adjustment physics, artificial heating is introduced prior to dynamic core, increasing temperature and enhancing surface convergence during dynamic core. This process ultimately strengthens the ITCZ, as illustrated in Fig. 2**d**.

In contrast, separating the computation and application of the nudging tendency by radiation transfer (*e.g.*, RNDG versus Z22) appears to have limited impact on model output. This difference stems from the intrinsic nature of adjustment physics versus radiation transfer. From the perspective of the Earth's energy budget, radiation acts to relax the climate toward an equilibrium state, as in the approximation widely used in classic studies such as Held and Hou (1980). As a result, biases introduced by nudging tend to be dampened by radiation transfer. In contrast, adjustment physics tends to modify the climate in a unidirectional manner—by removing moisture and heating the atmosphere—which can lead to the errors under certain nudging strategy (*i.e.*, DNDG). The contrasting roles of adjustment physics and radiation transfer explain why significant biases may arise under some nudging scheme but not others.

The difference between UVQ and UVT simulations, specifically the random precipitation pattern observed in the UVT simulation, arises from the decoupling of wind and moisture. Since the UV in baseline simulations does not exactly match CTLs, small biases in circulation can induce errors in specific humidity, which in turn affects precipitation during convection events. This issue also appears in the UV simulation (Fig. B2**a**). The time series of grid-scale precipitation from UVQ simulation closely matches that from CTLs, whereas nudging only the horizontal wind—as in the UV simulation—results in random deviations (Fig. B2**b**). However, as shown in Fig. 5**c**, when the model is nudged toward reanalysis data, these small-scale random errors are overshadowed by the dominant systematic bias and negligible in long-term mean.

In summary, the revised nudging schemes produce a climate that is more consistent with CTLs compared to the default strategy in CESM2.2.2. The relative differences in global means for precipitation, cloud cover, and low-level moisture are

https://doi.org/10.5194/egusphere-2025-2684
Preprint. Discussion started: 15 July 2025

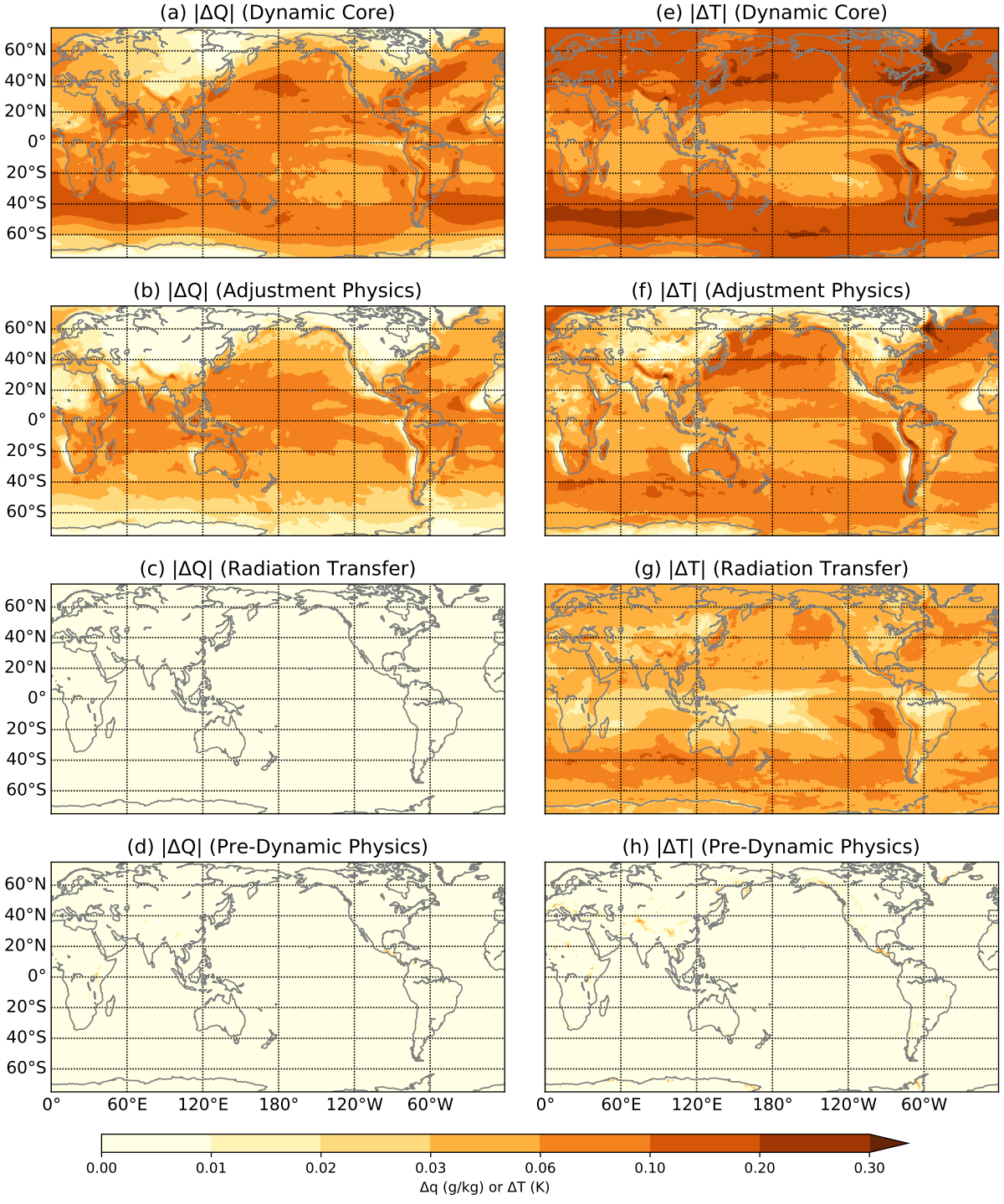

Figure 3. The 3-month mean of absolute changes in specific humidity (Q; left column) and temperature (T; right column) on about "859.5 mb" (in CESM2's hybrid sigma-pressure coordinate) due to different processes: (**a**, **e**) Dynamic Core, (**b**, **f**) Adjustment Physics, (**c**, **g**) Radiation Transfer, and (**d**, **f**) Pre-Dynamic Physics. Data is from CTLs simulation.

https://doi.org/10.5194/egusphere-2025-2684
Preprint. Discussion started: 15 July 2025

significantly reduced in RNDG (Fig. 4**a**), and the biases in both global patterns and time series are smaller than those observed with the default nudging scheme (Fig. 4**b** and **c**). Notably, temperature biases remain similar across nudging simulations regardless of whether temperature is nudged (UVT) or not (UVQ), whereas humidity biases are significantly reduced when specific humidity is directly nudged. This again reflects the small-scale random errors in UVT simulation as mentioned above. Based on the above discussion, to minimize potential errors due to the implementation of nudging, it is recommended to compute and apply the nudging tendency at the same point in the computing sequence of the climate model. At a minimum, the computation and application should not be separated by the adjustment physics stage. The subsequent discussion on nudging simulations will therefore focus on RNDG.

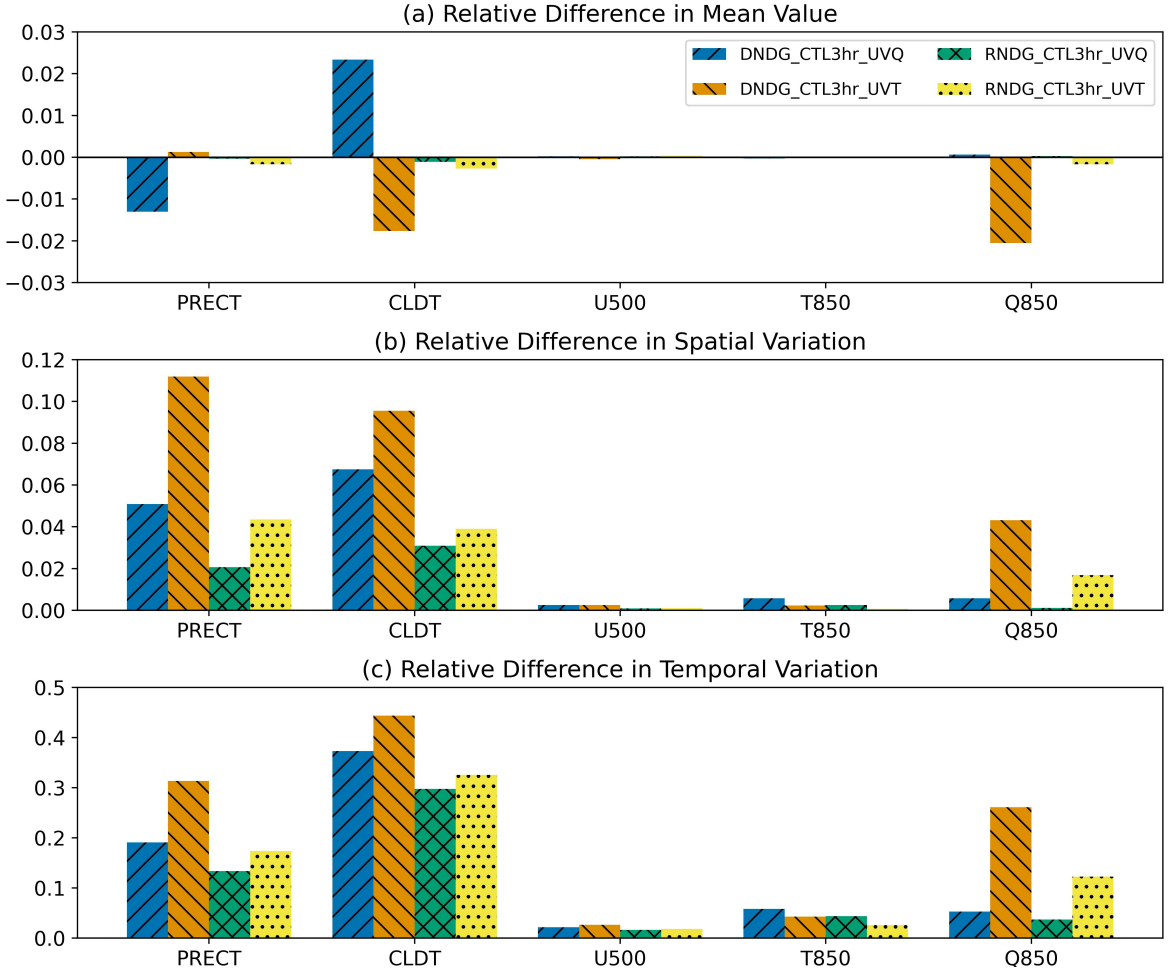

Figure 4. Comparison of total precipitation, total cloud, U at 500 mb, T at 850 mb, and Q at 850 mb between the baseline simulations and CTLs for (**a**) the difference in 3-month and global mean, (**b**) the deviation in global pattern of 3-month mean, and (**c**) the global mean of deviation in temporal evolution. All values are normalized by corresponding values in CTLs. See Appendix A for more details on how they are computed.

https://doi.org/10.5194/egusphere-2025-2684
Preprint. Discussion started: 15 July 2025

3.2 Evaluating precipitation bias using nudging

In previous studies, the nudging coefficient was typically set to values less than 0.1 (*i.e.*, a relaxation timescale longer than 5 hours) to prevent excessively strong nudging tendencies that could disrupt the dynamics of the model. However, to investigate the precipitation behavior of CESM2.2.2 under a "perfect" large-scale environment, we conducted a series of nudging simulations with a coefficient of 1 to ensure that all differences in the nudged variables between the model and the interpolated reanalysis data are eliminated at the end of each timestep (*i.e.*, when the model outputs the atmospheric state). The following discussion focuses on the tropical Pacific Ocean, where the double-ITCZ problem is observed.

Fig. 5 presents the 5-year climatology of IMERG precipitation and the difference between IMERG and the model simulations. In IMERG, the ITCZ in the eastern Pacific is located between 5°N and 12°N, accompanied by a much weaker precipitation band near 5°S (Fig. 5**a**). The CTL simulation exhibits a drier climate over the Pacific warm pool and the northern ITCZ region, with precipitation deficits exceeding 2 mm/day in the Pacific warm pool (Fig. 5**b**). In contrast, it shows a wet bias in the central tropical Pacific and subtropics. In the nudging simulations, when only horizontal wind is nudged toward reanalysis (RNDG_UV1; Fig. 5**c**), the overall precipitation bias is notably reduced. In most subtropical regions, the absolute difference in precipitation is less than 1 mm/day. The dry bias over the warm pool is alleviated, and a wet bias emerges along the northern ITCZ. When temperature is additionally nudged along with horizontal wind (RNDG_UVT1; Fig. 5**e**), the northern ITCZ becomes even wetter, while the warm pool becomes drier compared to RNDG_UV1. In the simulation where specific humidity is nudged alongside horizontal wind (RNDG_UVQ1; Fig. 5**d**), the dry bias over the warm pool persists at a similar magnitude to that in RNDG_UV1, but a prominent wet bias appears south of the equator.

Further analysis of precipitation characteristics by frequency and intensity is presented in Fig. 6 for three key regions: the western tropical Pacific warm pool, and the northern and southern ITCZ belts, as marked by the black boxes in Fig. 5**a**. In the warm pool, the contribution of hourly precipitation to the total amount peaks around 0.4 mm in CTL, while IMERG shows a peak near 2.8 mm (Fig. 6**d**). Nudging the model toward observed horizontal wind results in a distribution shape that resembles IMERG; however, the entire distribution is located at lower intensities, indicating an overall underestimation of heavier precipitation events. In the northern ITCZ belt, the nudging simulations increase the frequency of heavier precipitation relative to CTL, suggesting some improvement (Fig. 6**e**). Nonetheless, significant biases remain when compared to IMERG: light precipitation events ($\sim$1 mm) are still overly frequent, and heavy precipitation ($>$5 mm) remains substantially underestimated. In the southern ITCZ belt, nudging horizontal wind alone (UV) or together with temperature (UVT) effectively reduces the excessive drizzle and light precipitation present in CTL, thereby improving the shape of the amount distribution (Fig. 6**f**). However, nudging specific humidity (UVQ) leads to an overestimation of precipitation in the range of 0.1–0.6 mm compared to IMERG. Moreover, none of the nudging simulations adequately reproduce the contribution of heavy precipitation events. Similar features are observed in the distribution of daily precipitation, as shown in Fig. B4.

These results, along with the higher fraction of "No Rain" events in IMERG (Fig. 6**a**–**c**), reinforce previous findings that climate models tend to produce excessive drizzle (Dai, 2006; Fiedler et al., 2020), but they also offer new insights into the

https://doi.org/10.5194/egusphere-2025-2684
Preprint. Discussion started: 15 July 2025

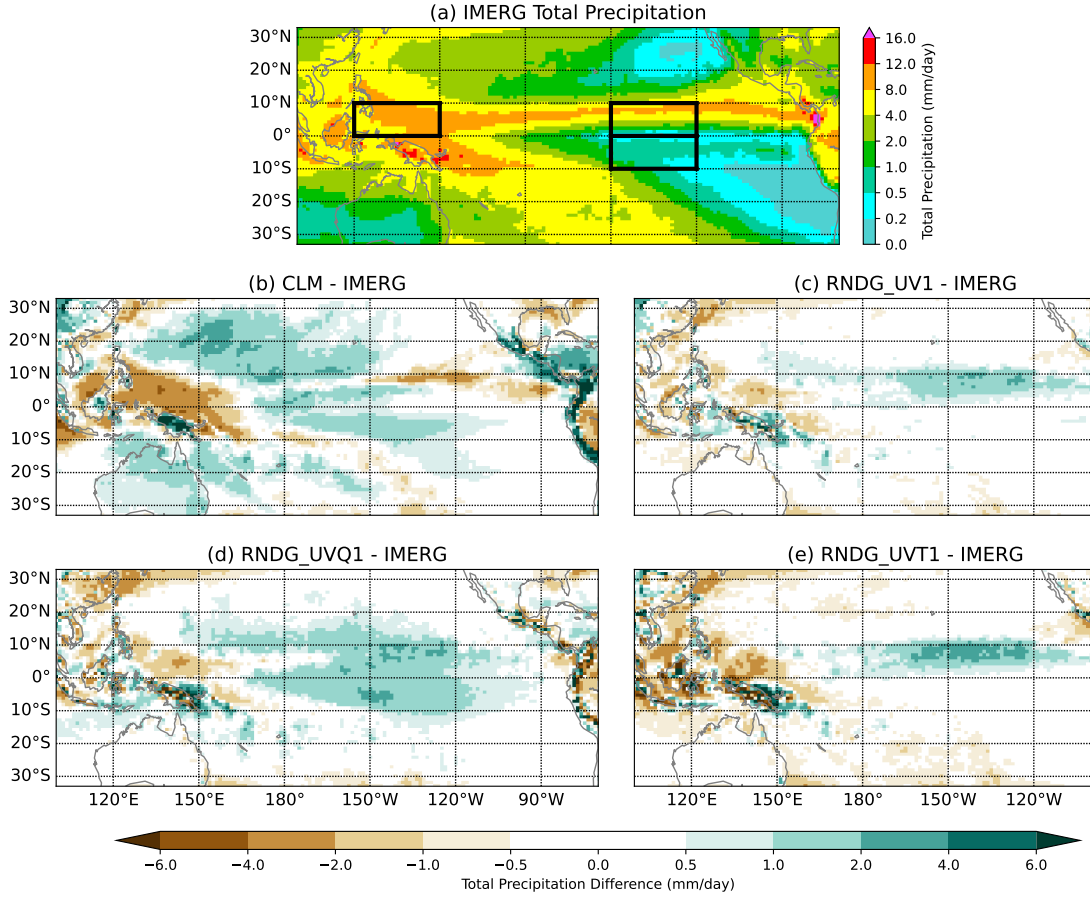

Figure 5. Climatological precipitation from (**a**) IMERG and (**b**–**e**) its differences to CTL and nudging simulations over the tropical Pacific Ocean during 2010–2014.

nature of modeled precipitation biases. By replacing the modeled circulation with 3-hourly reanalysis, the 5-year precipitation climatology from nudging simulation is more close to observation in terms of spatial pattern and mean value compared to CTL, suggesting that model's parameterizations are able to condense comparable amount of water vapor to rainfall in the long-term mean. However, this improved spatial pattern and mean-value is accompanied by a biased precipitation distribution, indicating unrealistic ways that water vapor is condensed. Since modeled precipitation comprises both convective and large-scale components, we further examine their respective contributions to the precipitation amount distribution, as shown in Fig. 7. Nudging toward reanalysis enhances the occurrence of heavier convective precipitation (>1 mm) across all three regions. Nonetheless, a clear limitation appears in regions with strong convection. In the northern ITCZ belt (Fig. 7**b**), the contribution of convective precipitation sharply declines at intensities above 1–3 mm, and virtually no convective events exceeding 5 mm are generated in any simulation. The majority of heavy precipitation instead originates from large-scale processes, such as stratiform macro-microphysics schemes, though the total amount remains well below that observed in IMERG (Fig. 7**d**–**f**).

https://doi.org/10.5194/egusphere-2025-2684
Preprint. Discussion started: 15 July 2025

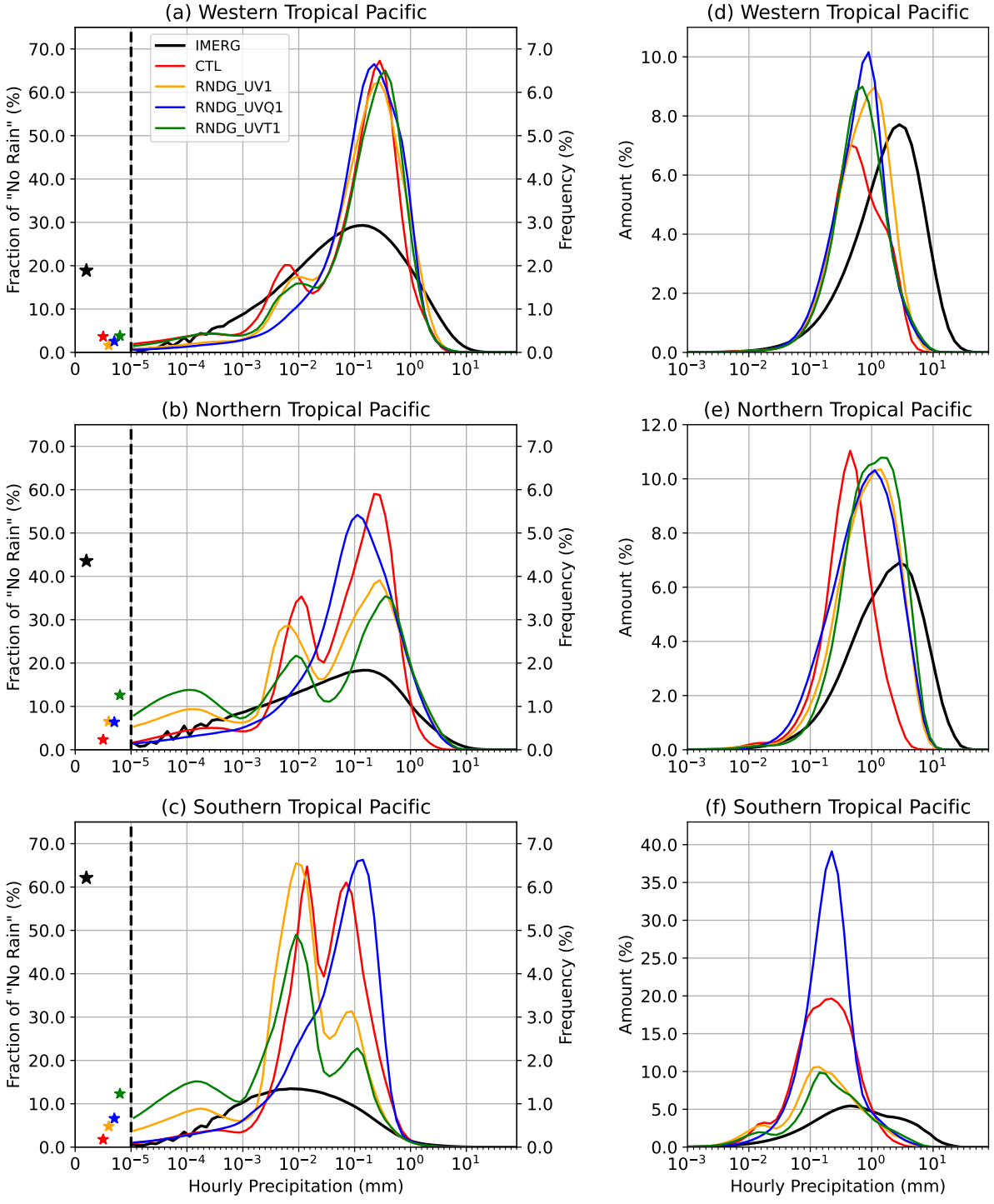

Figure 6. Composite distribution of hourly precipitation by frequency (left column) and amount (right column) in IMERG and simulations over three representative regions: (**a**, **d**) the western tropical Pacific, (**b**, **e**) the northern belt of ITCZ, and (**c**, **f**) the southern belt of ITCZ. "No Rain" means hourly precipitation less than 10^{-5} mm, and the fraction of no-precipitation is shown by stars to the left. For the right column, the amount in percent is normalized by IMERG total precipitation in each region. The x ticks are 10^[-5, -4.9, -4.8, ..., 2].

https://doi.org/10.5194/egusphere-2025-2684
Preprint. Discussion started: 15 July 2025

The contribution of stratiform macro-microphysics schemes to large-scale precipitation is also evident in the example time series shown in Fig. B6.

Although nudging UVQ generates the largest bias in the southern belt of the ITCZ, it produces the most reasonable probability distribution function (PDF) of hourly precipitation. As shown in Fig. 6**a**–**c**, the PDF of precipitation from CTL consistently shows three peaks, roughly around 0.1, 0.01, and 0.0001 mm, and a similar pattern is observed in the PDF based on daily precipitation (see Fig. B4). This feature is not observed in analyses of AMIP5 and AMIP6 in previous studies, such as Fig. 5 in Zhou et al. (2022). In contrast, the precipitation from IMERG exhibits a single-peak distribution across all three regions.

Fig. B5 provides more details on the PDF of precipitation for two grid boxes in the northern belt of the ITCZ. For both grid boxes, precipitation from IMERG exhibits a clear, single-peak distribution in each season, although they differ in intensity and magnitude of the peak. However, the precipitation from the free-running simulation shows two notable features: 1) the occurrence of the peak intensity is overly frequent in both summer and autumn, while other intensities occur too infrequently, and 2) at 2.4°N, 135°W, the peaks are concentrated around two intensity regimes, 0.01 and 0.1 mm. These two features are consistent with the multiple peaks observed in the PDF of regional composite precipitation shown in Fig. 6.

The climate differences between nudging and free-running simulations further highlight the model parameterization's failure to generate heavy precipitation. As shown in Fig. 8**b**, the observed horizontal wind (almost identical to RNDG_UV1 by definition) exhibits stronger low-level convergence at 950 mb over the eastern and western tropical Pacific compared to CTL. The enhanced convergence in RNDG_UV1 lead to stronger convection which is also evident by a warmer upper troposphere and lower OLR (Fig. 8**a**) compared to CTL, and the distribution of both convective and large-scale precipitation shifts toward heavier intensity in the northern tropical Pacific (Fig. 7**b** and **e**). However, the amount of heavy precipitation in nudging simulation is still lower than IMERG although with a higher regional average (Fig. 5**c**). In addition, this enhanced low-level convergence is associated with a higher vertically integrated water vapor compared to both CTL and reanalysis (Fig. 8**b** and **c**), indicating that the model's ability to condense water vapor is too low. Furthermore, when the modeled specific humidity is replaced with reanalysis in RNDG_UVQ1, the upper-level temperature drops to a level similar to CTL but lower than observation. This suggests that, given the same water vapor supply, the model requires a cooler troposphere to condense water. This finding aligns with previous studies reporting a significantly drier climate when UVQT is nudged (Ma et al., 2015), and similar result is shown in Fig. 9**e**.

The model's inefficiency in condensing water vapor is further evidenced by the relative humidity patterns shown in Fig. 9. In the nudging simulations, precipitation events generally occur in sync with observations, allowing for a direct comparison of atmospheric conditions during rainfall. To assess the model's moist process response, we output relative humidity at each timestep immediately after the moist physics but before the application of nudging, and compare it with observation during rainy hours when the hourly precipitation is larger than 1 mm in both simulations and IMERG. Strikingly, in the first three nudging experiments (UV, UVQ, and UVT; Fig. 9**a**–**c**), the simulated relative humidity during rainy hours exceeds that of the reanalysis across regions with 3-month mean precipitation greater than 5 mm/day, with the northern ITCZ belt exhibiting

https://doi.org/10.5194/egusphere-2025-2684
Preprint. Discussion started: 15 July 2025

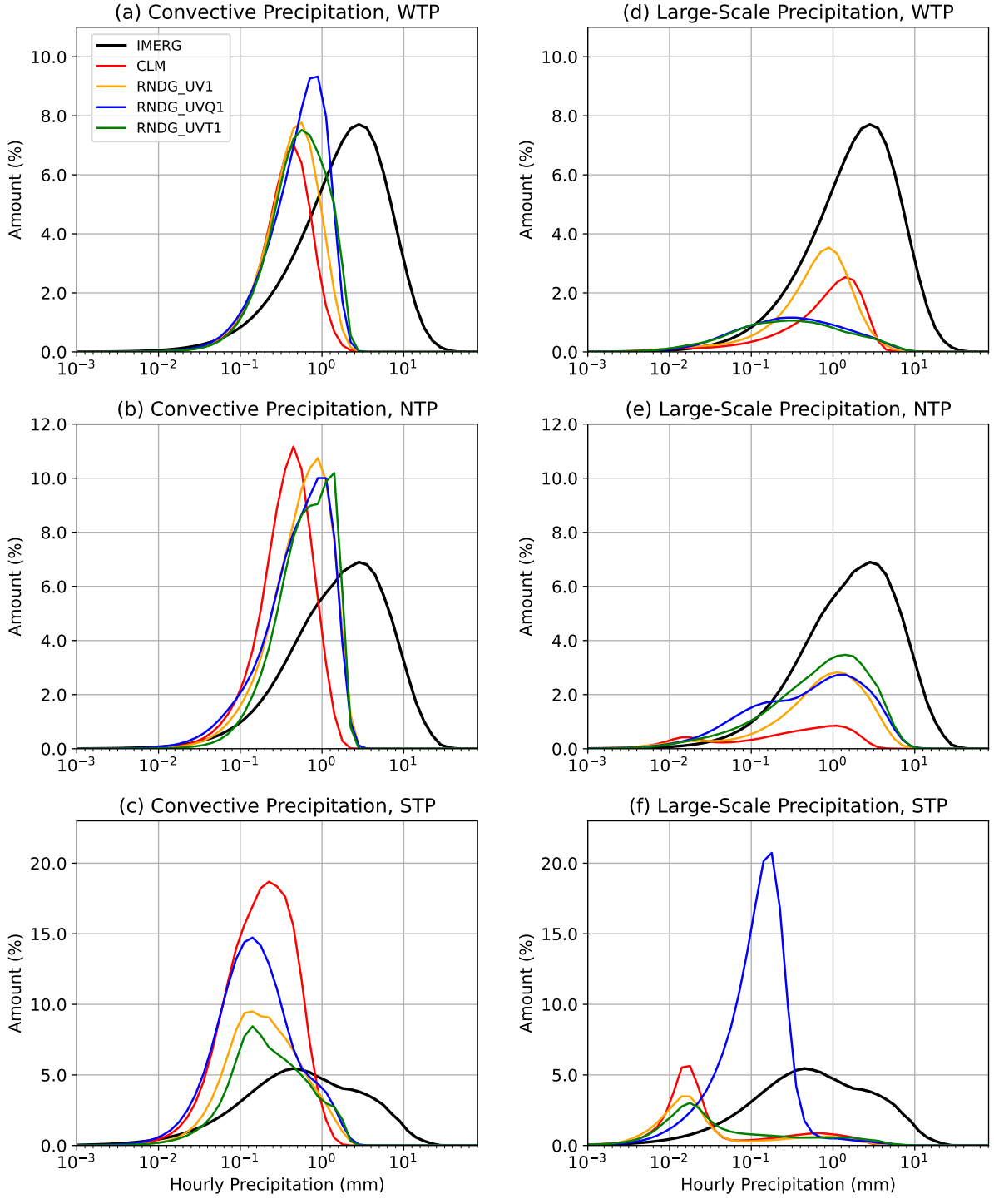

Figure 7. The same as the right column in Fig. 6 but for convective precipitation (left) and large-scale precipitation (right) from simulations. IMERG precipitation is shown as a reference.

https://doi.org/10.5194/egusphere-2025-2684
Preprint. Discussion started: 15 July 2025

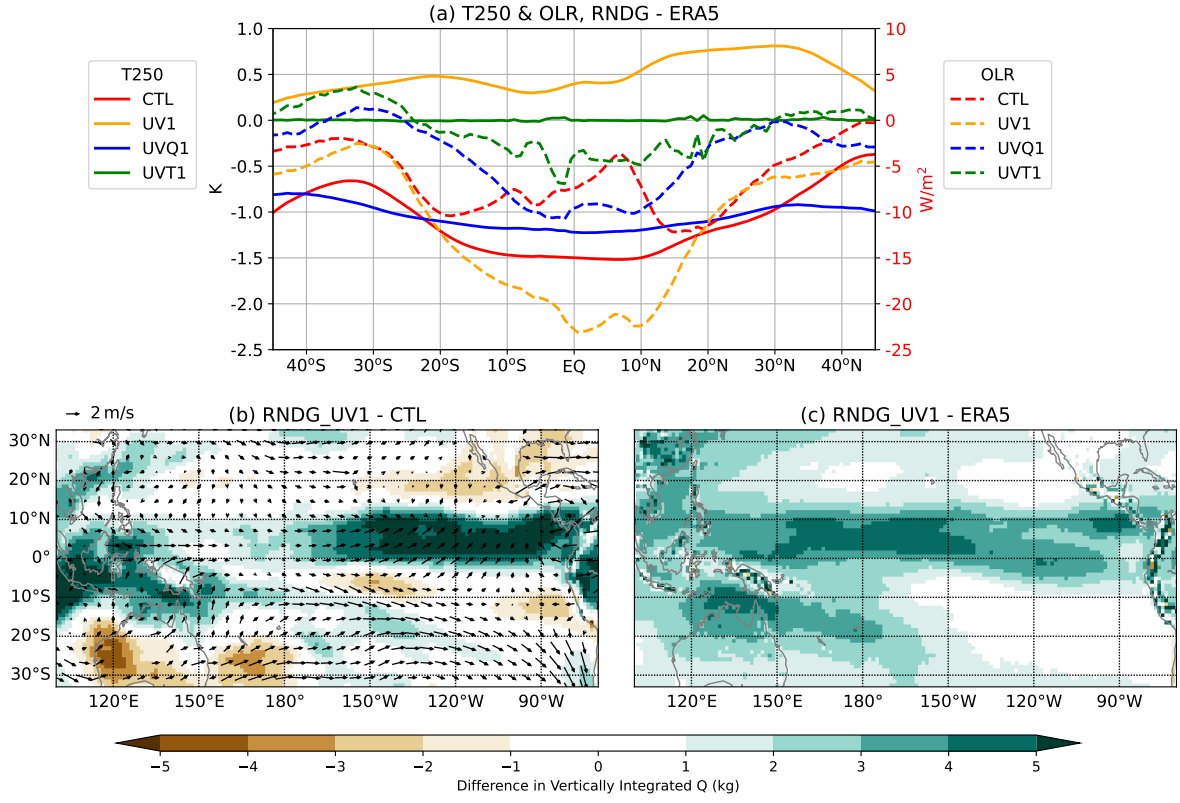

Figure 8. Climate difference between simulations and ERA5 during 2010–2014. (**a**) The difference in zonal mean 250 mb temperature (solid line) and OLR (dashed line) between 120°E and 120°W. (**b**) The difference in 950 mb horizontal winds and vertically integrated water vapor between RNDG_UV1 and CTL. (**c**) The difference in vertically integrated water vapor between RNDG_UV1 and ERA5. Note that the horizontal winds in nudging simulations are identical to ERA5, and the tropospheric temperature in RNDG_UVT1 is identical to ERA5.

differences as large as 6%. Even in the RNDG_UVQT1 simulation, where total precipitation is significantly lower than in IMERG, the relative humidity during rainy periods remains consistently higher than reanalysis (Fig. 9**d**). These results suggest that, given the input of atmospheric state at the beginning of model timestep, the model's parameterization schemes leave a moister atmosphere compared to reanalysis after conducting precipitation over one step. In other words, despite adequate moisture convergence—enforced through nudging—the model struggles to condense water vapor efficiently, highlighting a fundamental deficiency in its moist process representation.

4 Conclusions

In this study, we evaluate a fundamental role of moist parameterizations in GCMs—how well does the parameterization schemes simulate precipitation given the correct large-scale inputs? Inspired by Sun et al. (2019) and Zhang et al. (2022),

https://doi.org/10.5194/egusphere-2025-2684
Preprint. Discussion started: 15 July 2025

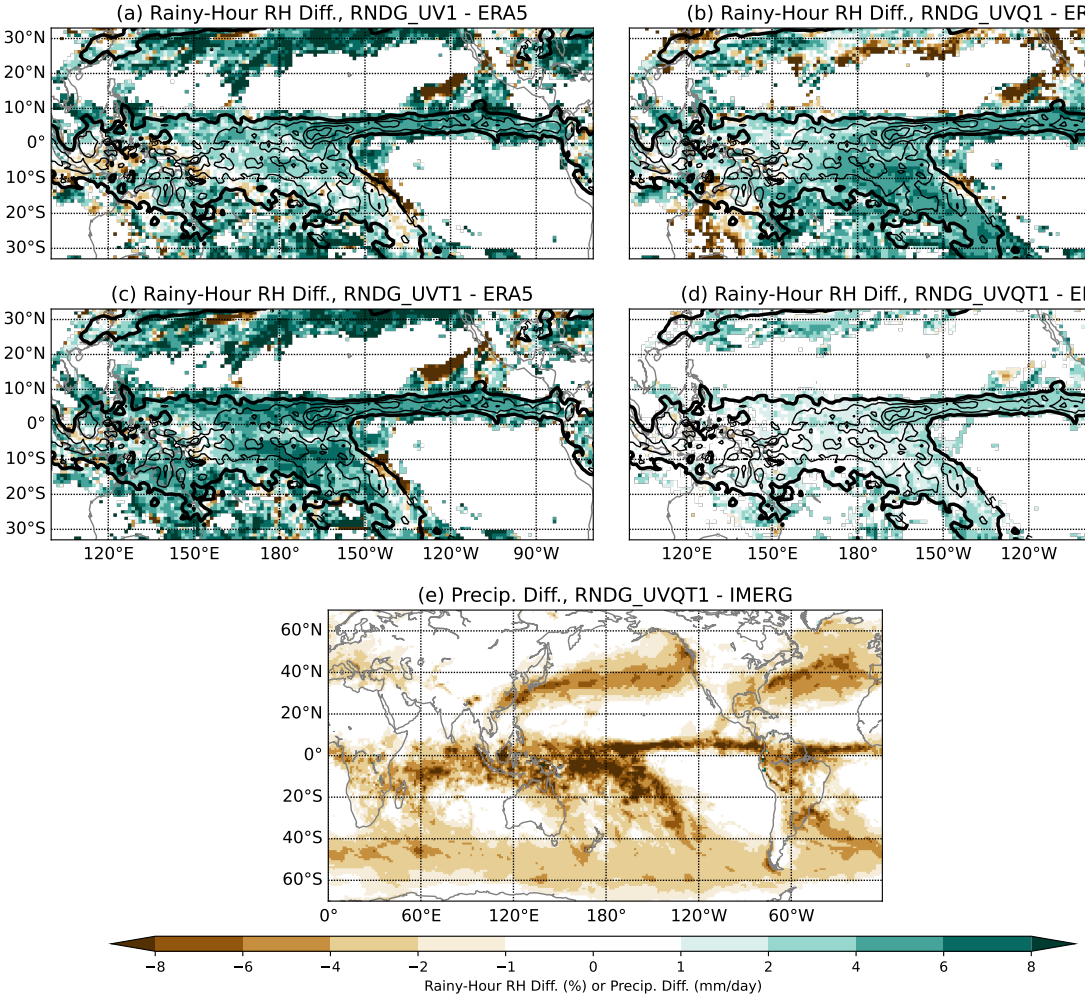

Figure 9. Difference in (**a**-**d**) 850 mb rainy-hour relative humidity (RH) between simulations and observation (ERA5) and (**e**) precipitation bias in RNDG_UVQT1 based on hourly outputs from 2010-01 to 2010-03. The rainy-hour is defined as the time when the hourly precipitation from both IMERG and a specific nudging simulation (RNDG_UV1 in **a**, RNDG_UVQ1 in **b**, RNDG_UVT1 in **c**, and RNDG_UVQT1 in **d**) is larger than 1 mm. The black contours represent 3-month averaged precipitation in IMERG starting from 5 mm/day (bold) and with an interval of 5 mm/day.

https://doi.org/10.5194/egusphere-2025-2684
Preprint. Discussion started: 15 July 2025

we firstly investigate how the choice of the nudging sequence and nudged variables affects precipitation behavior with the aim of developing an optimal nudging scheme for CESM2.2.2. By nudging the model to its own climate, we show that the default nudging sequence in CESM2.2.2 produces substantial precipitation errors (Fig. 2**b**–**d**). This bias primarily stems from an inconsistency where the computation and application of the nudging term is executed at different stages of model's integration. In regions where the physics of precipitation is frequently triggered, this separation causes excessive moisture removal (when humidity is nudged) and/or latent heat release (when temperature is nudged), leading to systematic biases in climatological precipitation. Across all four revised nudging schemes, the model exhibits less deviation in precipitation and other climate variables from the free-running simulation. An appropriate nudging scheme requires that, at a minimum, the computation and application of nudging should not be separated by the adjustment physics.

Next, we nudge the model toward reanalysis data, which allows us to dissect the model's precipitation biases into two parts—a part directly caused by the model's parameterizations and a part due to the feedbacks between the parameterizations and the large-scale environment. While we do not discuss the impact of parameterizations on the large-scale circulation, we expect the improvement of the former to benefit the latter, given the fact that precipitation and circulation are closely connected in GCMs (Lu et al., 2023; He et al., 2024).

Without nudging, the CTL simulation exhibits a negative precipitation bias in the Pacific warm pool and cold tongue, along with weaker low-level convergence, but a wetter subtropics. In addition, there is too much drizzle ($<$1 mm/hr) and insufficient heavy precipitation ($>$5 mm/hr) over the three selected regions: the warm pool and the northern/southern ITCZ. When the horizontal wind is replaced with reanalysis (RNDG_UV1), enhanced convergence supplies more water vapor to the eastern and western tropical Pacific, leading to an overall increase in precipitation. However, according to the frequency distribution of precipitation, RNDG_UV1 still produces too much drizzle and light precipitation through convection scheme and less heavy precipitation through stratiform macro-microphysics schemes. The lack of heavy precipitation can not be explained by excessive vapor consumption by convection scheme alone, as vertically integrated water vapor in RNDG_UV1 remains higher than in observations across the tropics. Nudging specific humidity (RNDG_UVQ1) yields little improvement in either the time-mean precipitation or its frequency distribution. In addition, when nudging simulations generally capture the precipitation events synchronously with observation, the modeled relative humidity is often larger during rainy hours, suggesting an inefficiency in the model's ability to condense moisture and generate precipitation.

Previous studies have emphasized the role of drizzle in modulating large-scale circulation and cloud radiative effects, particularly its contribution to the double-ITCZ problem. However, the direct impact of a model's precipitation parameterization has been difficult to isolate, as modeled precipitation is inherently coupled with the model's circulation and thermodynamic fields. In this study, we address this challenge by nudging the model toward reanalysis, thereby constraining large-scale dynamics and thermodynamics to observationally based states. This approach allows us to isolate the influence of precipitation parameterizations and provides a more detailed assessment of the model's ability to convert moisture into precipitation—beyond the commonly discussed drizzle issue. Our findings underscore the utility of nudging as a diagnostic tool for evaluating model behavior by decoupling parameterizations from large-scale variability. Nudging simulations can be viewed as an advanced

https://doi.org/10.5194/egusphere-2025-2684
Preprint. Discussion started: 15 July 2025

form of single-column modeling, specifically aimed at validating model parameterizations as demonstrated in earlier studies such as Zhang and McFarlane (1995), particularly with the support of modern computational resources.

Furthermore, as research increasingly examines the sensitivity of precipitation efficiency to greenhouse warming and its implications for climate change (Singh and O'Gorman, 2014; Lutsko and Cronin, 2018; Narsey et al., 2019; Li et al., 2022), biases in precipitation efficiency stemming from model parameterizations raise concerns about the reliability of GCMs' projections. Although the model can convert moisture into precipitation in terms of mean values—albeit with regional biases—the condensed water tends to fall as light rain too frequently due to shortcomings in the parameterizations. Such a bias may complicate the interpretation of changes in precipitation efficiency, particularly since parameterization schemes may respond differently under global warming. This study identifies a key limitation in current GCMs and highlights an important direction for future model development.

While nudging simulations provide a powerful means to constrain large-scale atmospheric states and isolate model deficiencies, the interpretation of nudging results depends on the accuracy of the reanalysis data used as the reference. In this study, ERA5 reanalysis is employed as the target for nudging horizontal wind (UV), temperature (T), and specific humidity (Q), while each of these fields contains intrinsic uncertainties and potential biases that may propagate into the simulations, thereby influencing the diagnosis of model behavior. Nevertheless, the conclusion regarding the model's inefficiency in converting moisture into precipitation remains qualitatively robust. For example, in the western tropical Pacific, nudging simulations consistently underestimate precipitation by 1/2 to 2/3 at similar percentiles when the intensity exceeds 1 mm/hr—a discrepancy that cannot be easily attributed to bias in the observed moisture supply. Future studies may consider using alternative reanalysis products to assess the sensitivity of nudging outcomes and further enhance the robustness of model evaluation.

Code and data availability. The ERA5 reanalysis data used in this study are deposited across 13 Zenodo repositories with Yang (2025n) for model evaluation and Yang (2025b, c, d, e, f, g, h, i, j, k, l, m) for nudging simulations, and are also available at ECMWF with DOI 10.24381/cds.bd0915c6 and 10.24381/cds/adbb2d47, respectively (Hersbach et al., 2023a, b). The IMERG precipitation is deposited across 5 Zenodo repositories (Yang, 2025o, p, q, r, s), and is also available at Goddard Earth Sciences Data and Information Services Center (GES DISC) with DOI 10.5067/GPM/IMERG/3B-HH/07 (Huffman et al., 2023). The CESM2.2.2 codes used for the climate model simulations is available at https://www.cesm.ucar.edu/models/cesm2 and is also provided on Zenodo with DOI 10.5281/zenodo.15857198 (Yang, 2025a) along with the run scripts and revised source codes for nudging. The post-processed model outputs from CESM2.2.2, processed reanalysis data, and the codes are available on Zenodo with DOI 10.5281/zenodo.15446770 (Yang et al., 2025).

https://doi.org/10.5194/egusphere-2025-2684
Preprint. Discussion started: 15 July 2025

Appendix A: Notes for Fig. 4

To compare climate conditions in the short-term simulations from Group 1, three types of relative differences are computed. The relative difference in mean value evaluates the difference in global- and time-mean values between the nudging and free-running simulations:

$$\text{Diff1} = \frac{[\overline{A_{EXP}}] - [\overline{A_{CTLs}}]}{[\overline{A_{CTLs}}]} \tag{A1}$$

where A is the variable of interest, EXP ($CTLs$) refers to the nudging (free-running) simulation, $\overline{A}$ denotes the 3-month average, and $[A]$ denotes the global average (area-weighted).

The relative difference in spatial variation quantifies differences in spatial patterns of time-mean fields:

$$\text{Diff2} = \frac{\text{RMSEs}(\overline{A_{EXPs}}^{*} - \overline{A_{CTLs}}^{*})}{\text{RMSEs}(\overline{A_{CTLs}}^{*})} \tag{A2}$$

where $A^{*} = A - [A]$ represents the anomaly relative to the global mean, and RMSEs(A) denotes the root-mean-square error of A over space.

The relative difference in temporal variation evaluates the global-mean differences in temporal variability of time series:

$$\text{Diff3} = \frac{[\text{RMSEt}(A'_{EXPs} - A'_{CTLs})]}{[\text{RMSEt}(A'_{CTLs})]} \tag{A3}$$

where $A' = A - \overline{A}$ denotes the anomaly relative to the time mean, and RMSEt(A) refers to the root-mean-square error of A over time.

https://doi.org/10.5194/egusphere-2025-2684
Preprint. Discussion started: 15 July 2025

Appendix B: Additional Figures

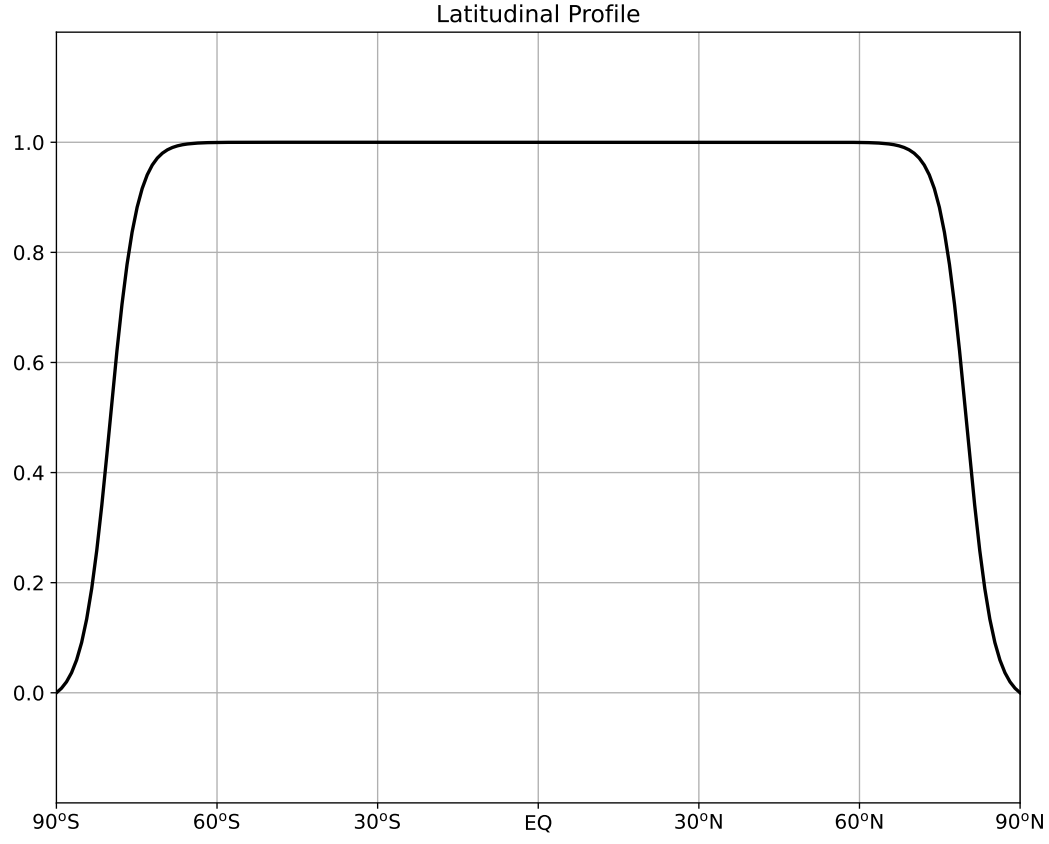

Figure B1. Latitudinal window-weighting for nudging tendency.

https://doi.org/10.5194/egusphere-2025-2684
Preprint. Discussion started: 15 July 2025

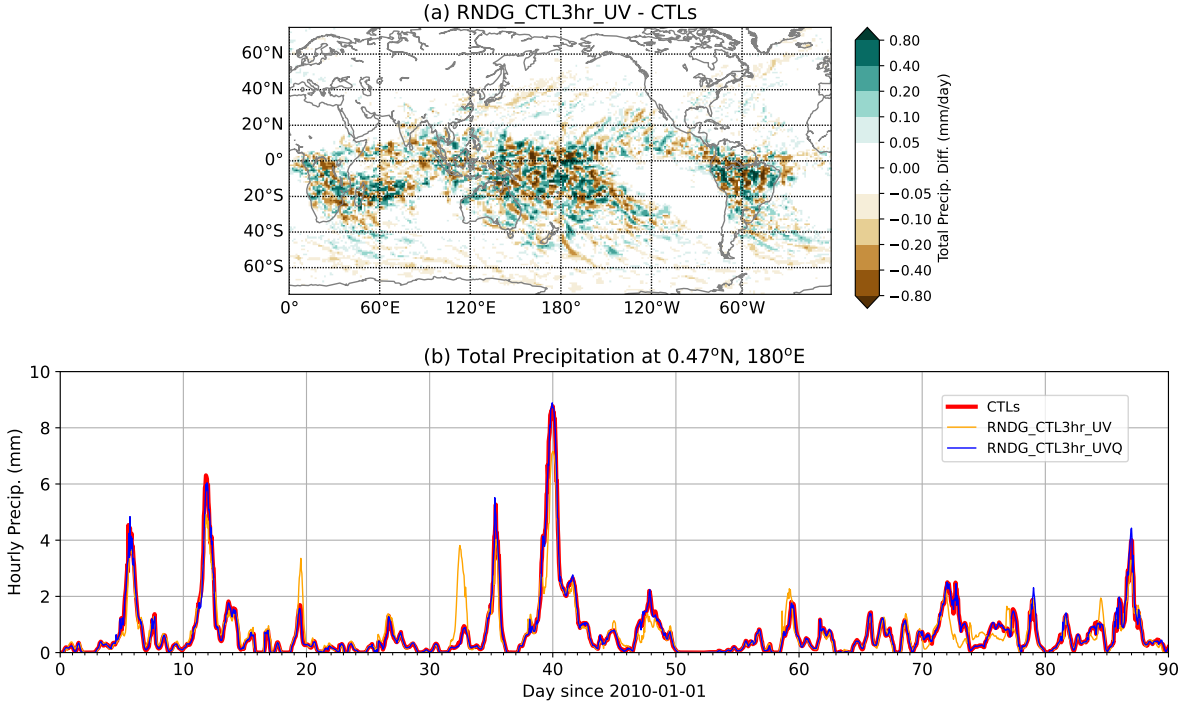

Figure B2. (**a**) The same as Fig. 2 but for UV-nudging simulations, and (**b**) the time series of total precipitation at 0.47°N, 180°E.

https://doi.org/10.5194/egusphere-2025-2684
Preprint. Discussion started: 15 July 2025

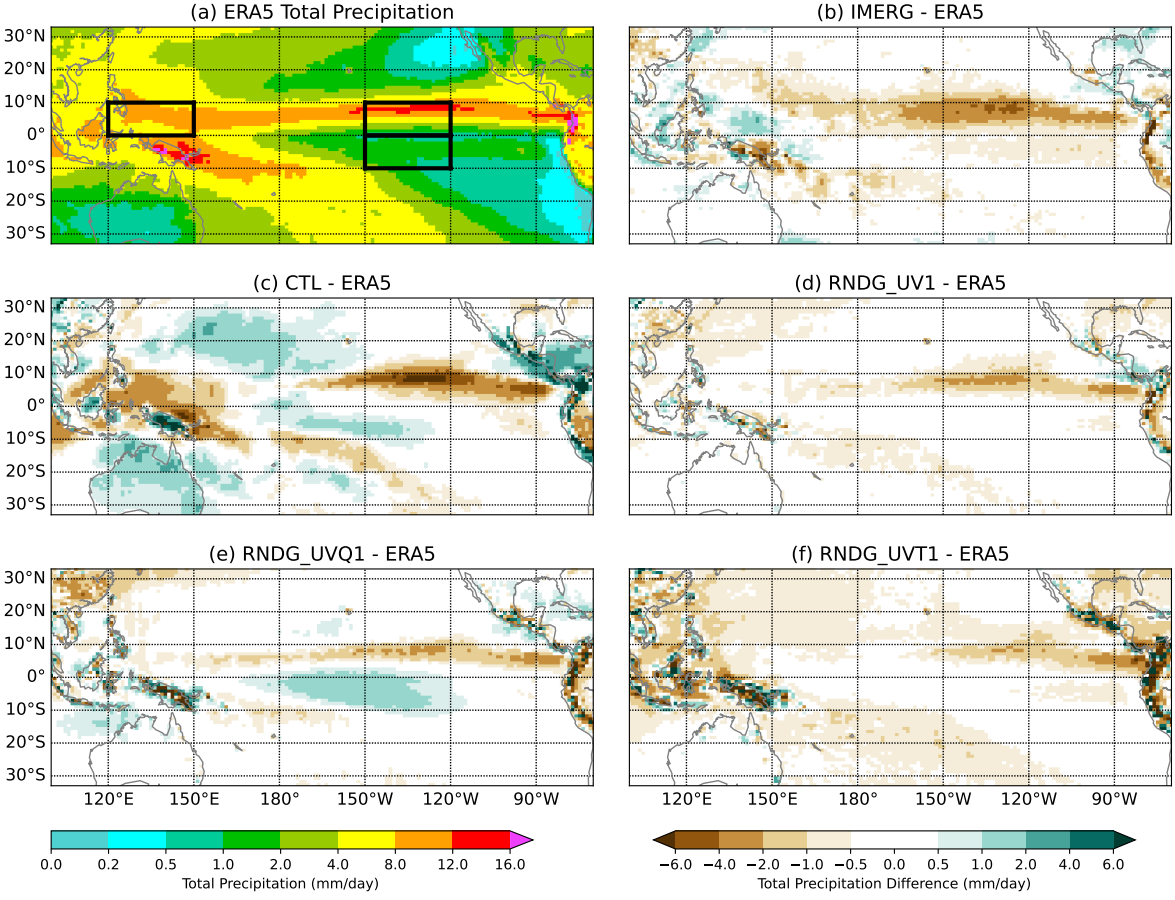

Figure B3. The same as Fig. 5 but with respect to ERA5 precipitation.

https://doi.org/10.5194/egusphere-2025-2684
Preprint. Discussion started: 15 July 2025

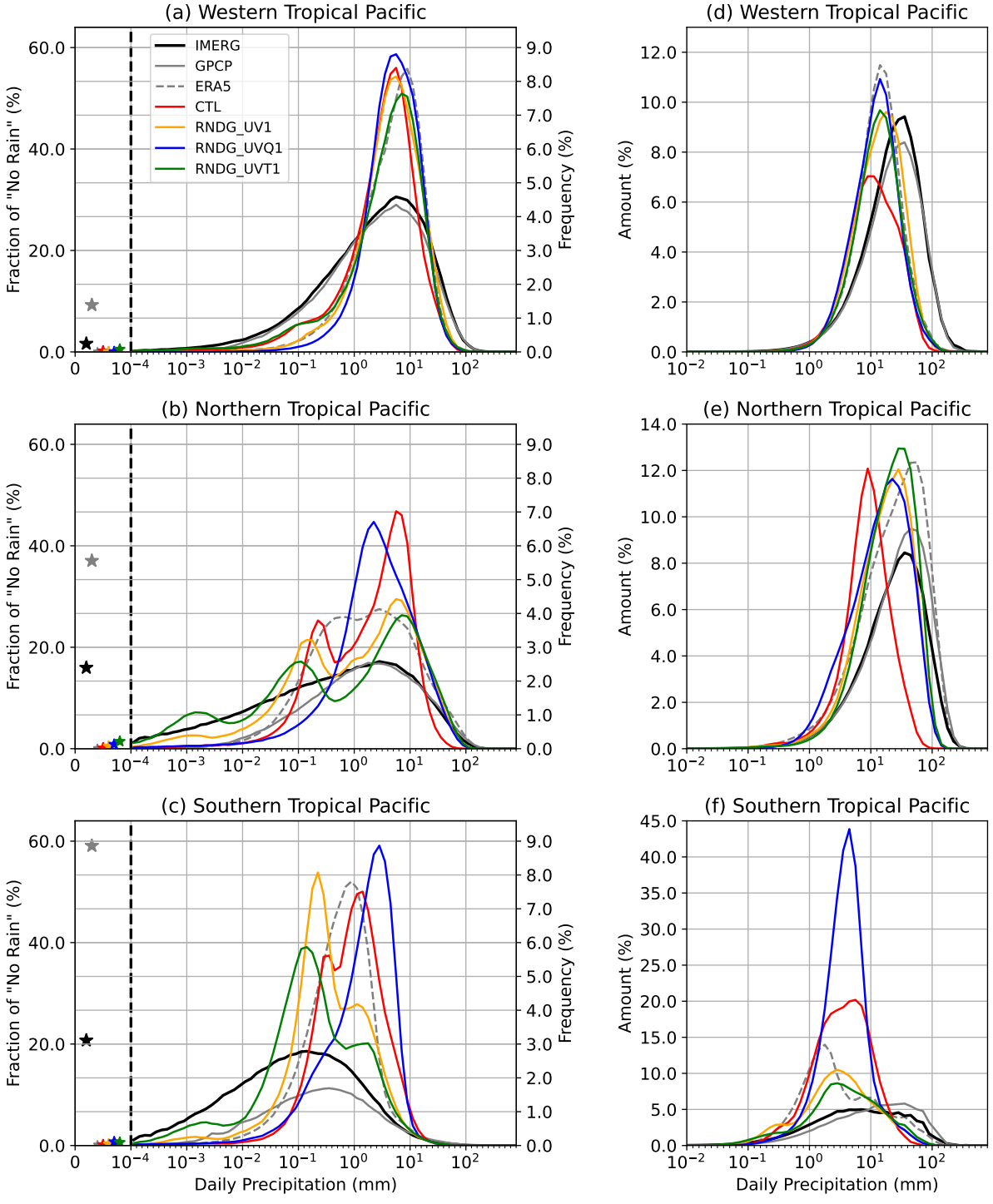

Figure B4. The same as Fig. 6 but for daily precipitation including ERA5 and GPCP data ("No Rain" is shown by a smaller grey star, which is the third from the left, for ERA5).

https://doi.org/10.5194/egusphere-2025-2684
Preprint. Discussion started: 15 July 2025

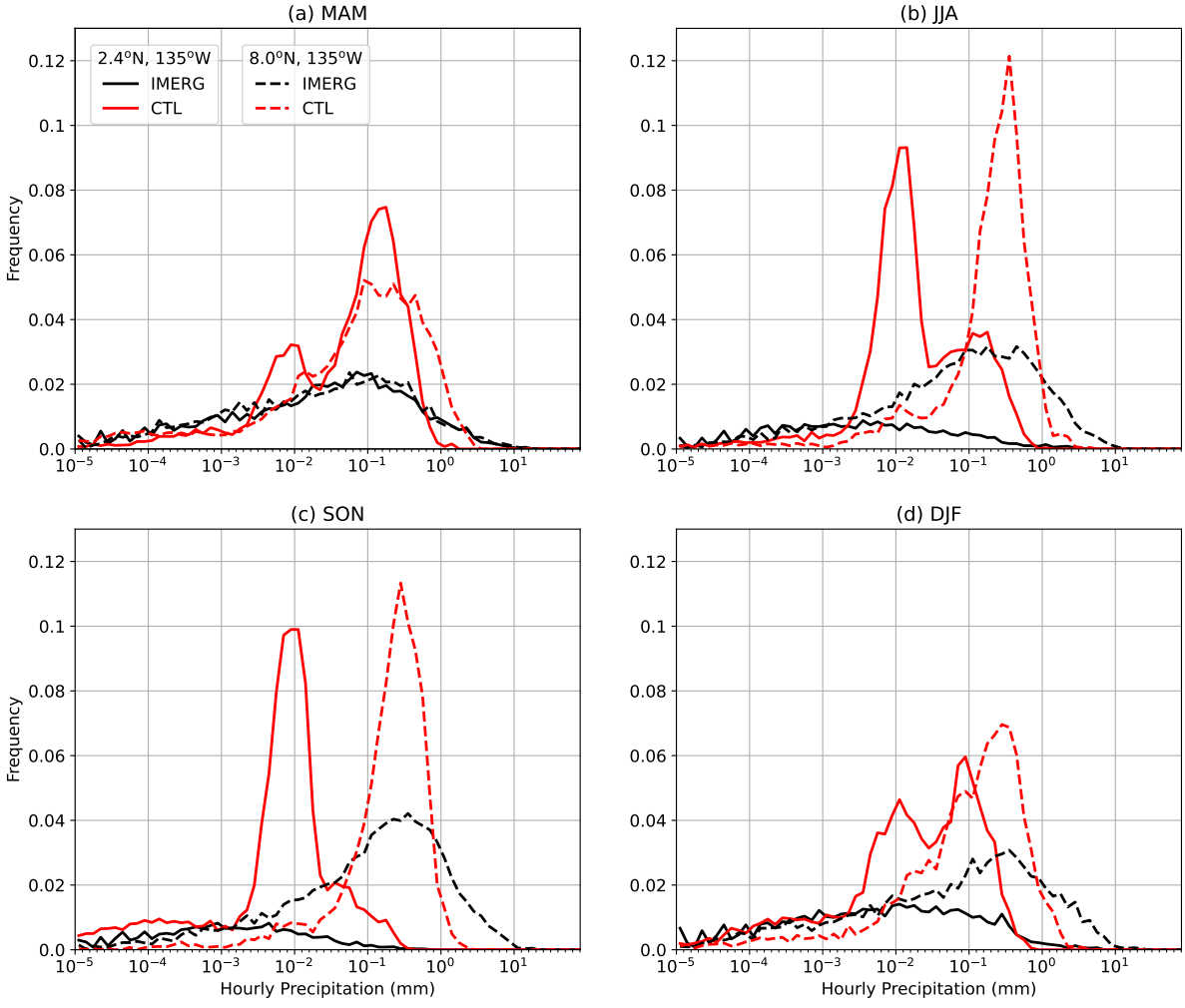

Figure B5. PDF of hourly precipitation from IMERG and free-running simulation (CLM) during different seasons, (**a**) spring (MAM), (**b**) summer (JJA), (**c**) autumn (SON), and (**d**) spring (DJF), on two grid boxes: 2.4°N, 135°W (solid line) and 8.0°N, 135°W (dashed line).

https://doi.org/10.5194/egusphere-2025-2684
Preprint. Discussion started: 15 July 2025

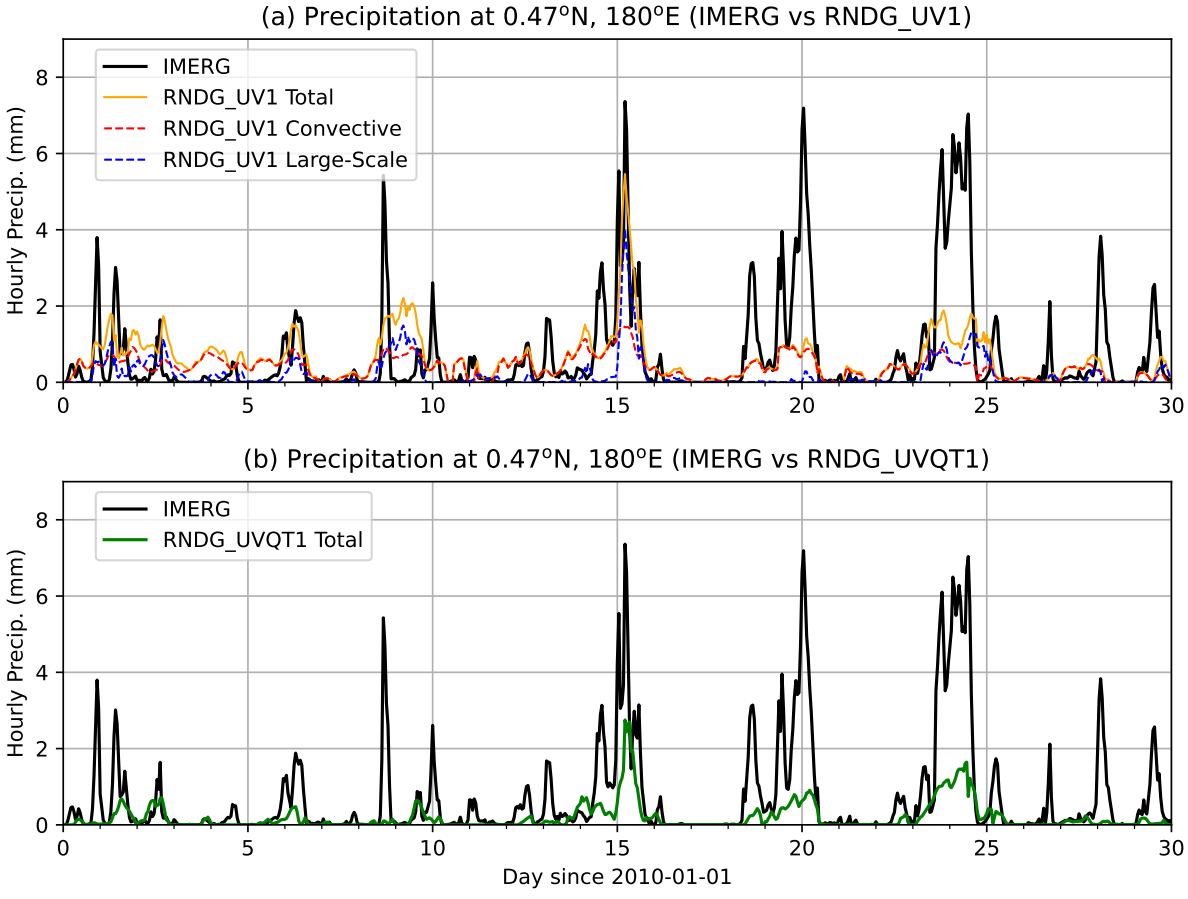

Figure B6. The time series of precipitation at 0.47°N, 180°E.

https://doi.org/10.5194/egusphere-2025-2684
Preprint. Discussion started: 15 July 2025

Author contributions. F.Y. and J.H. initiated this study. F.Y. conducted all the simulations, processed the model output, and carried out the analyses. F.Y. and J.H. wrote the paper. B.F., Y.-H.L., and Y.D. provided feedback. All the coauthors contributed to the revisions.

Competing interests. The authors declare that they have no conflict of interest.

Acknowledgements. Dr. Kezhou Lu at University of California, Los Angeles, is thanked for conceptualization at the beginning of this study and detailed comments improving the logic and organization of the manuscript. Dr. Guosheng Liu at Florida State University is thanked for discussions on the precipitation observation. We would like to acknowledge high-performance computing support from Derecho: HPE Cray EX System (DOI:10.5065/qx9apg09) provided by the National Center for Atmospheric Research's Computational and Information Systems Laboratory, sponsored by the National Science Foundation (NSF). F. Yang and J. He are supported by NSF grant AGS 2047270. B. Fosu and Y.-H. Lin are supported by NSF Awards AGS 2217619 and OAC 2321090. Y. Deng is supported by NSF through Grant AGS 2032532 and by National Oceanic and Atmospheric Administration (NOAA) through Grant NA22OAR4310606.

https://doi.org/10.5194/egusphere-2025-2684
Preprint. Discussion started: 15 July 2025

References

Bogenschutz, P. A., Gettelman, A., Morrison, H., Larson, V. E., Craig, C., and Schanen, D. P.: Higher-order turbulence closure and its impact on climate simulations in the Community Atmosphere Model, Journal of Climate, 26, 9655–9676, 2013.

Bony, S., Dufresne, J.-L., Le Treut, H., Morcrette, J.-J., and Senior, C.: On dynamic and thermodynamic components of cloud changes, Climate Dynamics, 22, 71–86, 2004.

Dai, A.: Precipitation characteristics in eighteen coupled climate models, Journal of Climate, 19, 4605–4630, 2006.

Fiedler, S., Crueger, T., D'Agostino, R., Peters, K., Becker, T., Leutwyler, D., Paccini, L., Burdanowitz, J., Buehler, S. A., Cortes, A. U., et al.: Simulated tropical precipitation assessed across three major phases of the coupled model intercomparison project (CMIP), Monthly Weather Review, 148, 3653–3680, 2020.

Gettelman, A. and Morrison, H.: Advanced two-moment bulk microphysics for global models. Part I: Off-line tests and comparison with other schemes, Journal of Climate, 28, 1268–1287, 2015.

Golaz, J.-C., Larson, V. E., and Cotton, W. R.: A PDF-based model for boundary layer clouds. Part I: Method and model description, Journal of the atmospheric sciences, 59, 3540–3551, 2002.

Gordon, C. T., Rosati, A., and Gudgel, R.: Tropical sensitivity of a coupled model to specified ISCCP low clouds, Journal of Climate, 13, 2239–2260, 2000.

Hawcroft, M., Haywood, J. M., Collins, M., Jones, A., Jones, A. C., and Stephens, G.: Southern Ocean albedo, inter-hemispheric energy transports and the double ITCZ: Global impacts of biases in a coupled model, Climate Dynamics, 48, 2279–2295, 2017.

He, J., Lu, K., Fosu, B., and Fueglistaler, S. A.: Diverging hydrological sensitivity among tropical basins, Nature Climate Change, 14, 623–628, 2024.

Held, I. M. and Hou, A. Y.: Nonlinear axially symmetric circulations in a nearly inviscid atmosphere, Journal of the Atmospheric Sciences, 37, 515–533, 1980.

Hersbach, H., Bell, B., Berrisford, P., Hirahara, S., Horányi, A., Muñoz-Sabater, J., Nicolas, J., Peubey, C., Radu, R., Schepers, D., et al.: The ERA5 global reanalysis, Quarterly Journal of the Royal Meteorological Society, 146, 1999–2049, 2020.

Hersbach, H., Bell, B., Berrisford, P., Biavati, G., Horányi, A., Muñoz Sabater, J., Nicolas, J., Peubey, C., Radu, R., Rozum, I., Schepers, D., Simmons, A., Soci, C., Dee, D., and Thépaut, J.-N.: [Dataset] ERA5 hourly data on pressure levels from 1940 to present, Copernicus Climate Change Service (C3S) Climate Data Store (CDS), https://doi.org/10.24381/cds.bd0915c6, 2023a.

Hersbach, H., Bell, B., Berrisford, P., Biavati, G., Horányi, A., Muñoz Sabater, J., Nicolas, J., Peubey, C., Radu, R., Rozum, I., Schepers, D., Simmons, A., Soci, C., Dee, D., and Thépaut, J.-N.: [Dataset] ERA5 hourly data on single levels from 1940 to present, Copernicus Climate Change Service (C3S) Climate Data Store (CDS), https://doi.org/10.24381/cds.adbb2d47, 2023b.

Hoke, J. E. and Anthes, R. A.: The initialization of numerical models by a dynamic-initialization technique, Monthly Weather Review, 104, 1551–1556, 1976.

Huffman, G. J., Bolvin, D. T., Braithwaite, D., Hsu, K.-L., Joyce, R. J., Kidd, C., Nelkin, E. J., Sorooshian, S., Stocker, E. F., Tan, J., et al.: Integrated multi-satellite retrievals for the global precipitation measurement (GPM) mission (IMERG), Satellite precipitation measurement: Volume 1, pp. 343–353, 2020.

Huffman, G. J., Stocker, E. F., Bolvin, D. T., Nelkin, E. J., and Tan, J.: [Dataset] GPM IMERG Final Precipitation L3 Half Hourly 0.1 degree x 0.1 degree V07, Goddard Earth Sciences Data and Information Services Center (GES DISC), https://doi.org/10.5067/GPM/IMERG/3B-HH/07, 2023.

https://doi.org/10.5194/egusphere-2025-2684
Preprint. Discussion started: 15 July 2025

Hwang, Y.-T. and Frierson, D. M. W.: Link between the double-Intertropical Convergence Zone problem and cloud biases over the Southern Ocean, Proceedings of the National Academy of Sciences, 110, 4935–4940, 2013.

Kang, S. M., Held, I. M., Frierson, D. M. W., and Zhao, M.: The response of the ITCZ to extratropical thermal forcing: Idealized slab-ocean experiments with a GCM, Journal of Climate, 21, 3521–3532, 2008.

Kay, J. E., Wall, C., Yettella, V., Medeiros, B., Hannay, C., Caldwell, P., and Bitz, C.: Global climate impacts of fixing the Southern Ocean shortwave radiation bias in the Community Earth System Model (CESM), Journal of Climate, 29, 4617–4636, 2016.

Lavers, D. A., Simmons, A., Vamborg, F., and Rodwell, M. J.: An evaluation of ERA5 precipitation for climate monitoring, Quarterly Journal of the Royal Meteorological Society, 148, 3152–3165, 2022.

Li, G. and Xie, S.-P.: Tropical biases in CMIP5 multimodel ensemble: The excessive equatorial Pacific cold tongue and double ITCZ problems, Journal of Climate, 27, 1765–1780, 2014.

Li, R. L., Studholme, J. H. P., Fedorov, A. V., and Storelvmo, T.: Precipitation efficiency constraint on climate change, Nature Climate Change, 12, 642–648, 2022.

Lin, G., Wan, H., Zhang, K., Qian, Y., and Ghan, S. J.: Can nudging be used to quantify model sensitivities in precipitation and cloud forcing?, Journal of Advances in Modeling Earth Systems, 8, 1073–1091, 2016.

Lin, J.-L.: The double-ITCZ problem in IPCC AR4 coupled GCMs: Ocean–atmosphere feedback analysis, Journal of Climate, 20, 4497–4525, 2007.

Lu, K., He, J., and Simpson, I. R.: Origins of uncertainty in the response of the summer north Pacific subtropical high to CO2 forcing, Geophysical Research Letters, 50, e2023GL105 042, 2023.

Lutsko, N. J. and Cronin, T. W.: Increase in precipitation efficiency with surface warming in radiative-convective equilibrium, Journal of Advances in Modeling Earth Systems, 10, 2992–3010, 2018.

Ma, C.-C., Mechoso, C. R., Robertson, A. W., and Arakawa, A.: Peruvian stratus clouds and the tropical Pacific circulation: A coupled ocean-atmosphere GCM study, Journal of Climate, 9, 1635–1645, 1996.

Ma, H.-Y., Chuang, C. C., Klein, S. A., Lo, M.-H., Zhang, Y., Xie, S., Zheng, X., Ma, P.-L., Zhang, Y., and Phillips, T. J.: An improved hindcast approach for evaluation and diagnosis of physical processes in global climate models, Journal of Advances in Modeling Earth Systems, 7, 1810–1827, 2015.

Mechoso, C. R., Robertson, A. W., Barth, N., Davey, M. K., Delecluse, P., Gent, P. R., Ineson, S., Kirtman, B., Latif, M., Le Treut, H., et al.: The seasonal cycle over the tropical Pacific in coupled ocean–atmosphere general circulation models, Monthly Weather Review, 123, 2825–2838, 1995.

Narsey, S., Jakob, C., Singh, M. S., Bergemann, M., Louf, V., Protat, A., and Williams, C.: Convective precipitation efficiency observed in the tropics, Geophysical Research Letters, 46, 13 574–13 583, 2019.

Omrani, H., Drobinski, P., and Dubos, T.: Using nudging to improve global-regional dynamic consistency in limited-area climate modeling: What should we nudge?, Climate Dynamics, 44, 1627–1644, 2015.

Rasch, P. J., Xie, S., Ma, P.-L., Lin, W., Wang, H., Tang, Q., Burrows, S. M., Caldwell, P., Zhang, K., Easter, R. C., et al.: An overview of the atmospheric component of the Energy Exascale Earth System Model, Journal of Advances in Modeling Earth Systems, 11, 2377–2411, 2019.

Singh, M. S. and O'Gorman, P. A.: Influence of microphysics on the scaling of precipitation extremes with temperature, Geophysical Research Letters, 41, 6037–6044, 2014.

https://doi.org/10.5194/egusphere-2025-2684
Preprint. Discussion started: 15 July 2025

Song, F. and Zhang, G. J.: Effects of southeastern Pacific sea surface temperature on the double-ITCZ bias in NCAR CESM1, Journal of Climate, 29, 7417–7433, 2016.

Song, X. and Zhang, G. J.: Convection parameterization, tropical Pacific double ITCZ, and upper-ocean biases in the NCAR CCSM3. Part I: Climatology and atmospheric feedback, Journal of Climate, 22, 4299–4315, 2009.

Song, X. and Zhang, G. J.: Reduction of Pacific double-ITCZ bias by convection parameterization in NCAR CESM2. 2, Journal of Advances in Modeling Earth Systems, 17, e2024MS004 309, 2025.

Subramanian, A. C. and Zhang, G. J.: Diagnosing MJO hindcast biases in NCAR CAM3 using nudging during the DYNAMO field campaign, Journal of Geophysical Research: Atmospheres, 119, 7231–7253, 2014.

Sun, J., Zhang, K., Wan, H., Ma, P.-L., Tang, Q., and Zhang, S.: Impact of nudging strategy on the climate representativeness and hindcast skill of constrained EAMv1 simulations, Journal of Advances in Modeling Earth Systems, 11, 3911–3933, 2019.

Tiedtke, M.: A comprehensive mass flux scheme for cumulus parameterization in large-scale models, Monthly weather review, 117, 1779–1800, 1989.

Vincent, C. L. and Hahmann, A. N.: The impact of grid and spectral nudging on the variance of the near-surface wind speed, Journal of Applied Meteorology and Climatology, 54, 1021–1038, 2015.

Woelfle, M. D., Bretherton, C. S., Hannay, C., and Neale, R.: Evolution of the double-ITCZ bias through CESM2 development, Journal of Advances in Modeling Earth Systems, 11, 1873–1893, 2019.

Yang, F.: [Dataset] Evaluating Precipitation Behavior in CESM2 Using Nudging Technique (Model Data), Zenodo, https://doi.org/10.5281/zenodo.15857198, 2025a.

Yang, F.: [Dataset] Evaluating Precipitation Behavior in CESM2 Using Nudging Technique (Nudging Data, 2009p1), Zenodo, https://doi.org/10.5281/zenodo.15857787, 2025b.

Yang, F.: [Dataset] Evaluating Precipitation Behavior in CESM2 Using Nudging Technique (Nudging Data, 2009p2), Zenodo, https://doi.org/10.5281/zenodo.15857998, 2025c.

Yang, F.: [Dataset] Evaluating Precipitation Behavior in CESM2 Using Nudging Technique (Nudging Data, 2010p1), Zenodo, https://doi.org/10.5281/zenodo.15858147, 2025d.

Yang, F.: [Dataset] Evaluating Precipitation Behavior in CESM2 Using Nudging Technique (Nudging Data, 2010p2), Zenodo, https://doi.org/10.5281/zenodo.15858157, 2025e.

Yang, F.: [Dataset] Evaluating Precipitation Behavior in CESM2 Using Nudging Technique (Nudging Data, 2011p1), Zenodo, https://doi.org/10.5281/zenodo.15858582, 2025f.

Yang, F.: [Dataset] Evaluating Precipitation Behavior in CESM2 Using Nudging Technique (Nudging Data, 2011p2), Zenodo, https://doi.org/10.5281/zenodo.15858539, 2025g.

Yang, F.: [Dataset] Evaluating Precipitation Behavior in CESM2 Using Nudging Technique (Nudging Data, 2012p1), Zenodo, https://doi.org/10.5281/zenodo.15858725, 2025h.

Yang, F.: [Dataset] Evaluating Precipitation Behavior in CESM2 Using Nudging Technique (Nudging Data, 2012p2), Zenodo, https://doi.org/10.5281/zenodo.15858723, 2025i.

Yang, F.: [Dataset] Evaluating Precipitation Behavior in CESM2 Using Nudging Technique (Nudging Data, 2013p1), Zenodo, https://doi.org/10.5281/zenodo.15858799, 2025j.

Yang, F.: [Dataset] Evaluating Precipitation Behavior in CESM2 Using Nudging Technique (Nudging Data, 2013p2), Zenodo, https://doi.org/10.5281/zenodo.15858832, 2025k.

https://doi.org/10.5194/egusphere-2025-2684
Preprint. Discussion started: 15 July 2025

Yang, F.: [Dataset] Evaluating Precipitation Behavior in CESM2 Using Nudging Technique (Nudging Data, 2014p1), Zenodo, https://doi.org/10.5281/zenodo.15858886, 2025l.

Yang, F.: [Dataset] Evaluating Precipitation Behavior in CESM2 Using Nudging Technique (Nudging Data, 2014p2), Zenodo, https://doi.org/10.5281/zenodo.15858902, 2025m.

Yang, F.: [Dataset] Evaluating Precipitation Behavior in CESM2 Using Nudging Technique (ERA5, single-level), Zenodo, https://doi.org/10.5281/zenodo.15864322, 2025n.

Yang, F.: [Dataset] Evaluating Precipitation Behavior in CESM2 Using Nudging Technique (IMERG part 1), Zenodo, https://doi.org/10.5281/zenodo.15865411, 2025o.

Yang, F.: [Dataset] Evaluating Precipitation Behavior in CESM2 Using Nudging Technique (IMERG part 2), Zenodo, https://doi.org/10.5281/zenodo.15865425, 2025p.

Yang, F.: [Dataset] Evaluating Precipitation Behavior in CESM2 Using Nudging Technique (IMERG part 3), Zenodo, https://doi.org/10.5281/zenodo.15866168, 2025q.

Yang, F.: [Dataset] Evaluating Precipitation Behavior in CESM2 Using Nudging Technique (IMERG part 4), Zenodo, https://doi.org/10.5281/zenodo.15866370, 2025r.

Yang, F.: [Dataset] Evaluating Precipitation Behavior in CESM2 Using Nudging Technique (IMERG part 5), Zenodo, https://doi.org/10.5281/zenodo.15866373, 2025s.

Yang, F., He, J., Fuso, B., Lin, Y.-H., and Deng, Y.: [Dataset] Evaluating Precipitation Behavior in CESM2 Using Nudging Technique, Zenodo, https://doi.org/10.5281/zenodo.15446770, 2025.

Yu, J.-Y. and Mechoso, C. R.: Links between annual variations of Peruvian stratocumulus clouds and of SST in the eastern equatorial Pacific, Journal of Climate, 12, 3305–3318, 1999.

Zhang, G. J. and McFarlane, N. A.: Sensitivity of climate simulations to the parameterization of cumulus convection in the Canadian Climate Centre general circulation model, Atmosphere-ocean, 33, 407–446, 1995.

Zhang, G. J. and Wang, H.: Toward mitigating the double ITCZ problem in NCAR CCSM3, Geophysical research letters, 33, 2006.

Zhang, G. J., Song, X., and Wang, Y.: The double ITCZ syndrome in GCMs: A coupled feedback problem among convection, clouds, atmospheric and ocean circulations, Atmospheric Research, 229, 255–268, 2019.

Zhang, K., Wan, H., Liu, X., Ghan, S. J., Kooperman, G. J., Ma, P.-L., Rasch, P. J., Neubauer, D., and Lohmann, U.: On the use of nudging for aerosol–climate model intercomparison studies, Atmospheric Chemistry and Physics, 14, 8631–8645, 2014.

Zhang, S., Zhang, K., Wan, H., and Sun, J.: Further improvement and evaluation of nudging in the E3SM Atmosphere Model version 1 (EAMv1): simulations of the mean climate, weather events, and anthropogenic aerosol effects, Geoscientific Model Development, 15, 6787–6816, 2022.

Zhang, X., Liu, H., and Zhang, M.: Double ITCZ in coupled ocean-atmosphere models: From CMIP3 to CMIP5, Geophysical Research Letters, 42, 8651–8659, 2015.

Zhou, W., Leung, L. R., and Lu, J.: Linking large-scale double-ITCZ bias to local-scale drizzling bias in climate models, Journal of Climate, 35, 7965–7979, 2022.